

## Supplementary Material, Methods, and Results

<b>Supplemental Material and Methods</b>	<b>1</b>
Objectives and methods overview	1
Samples	2
16p11.2 cohort	2
22q11.2 cohort	2
Idiopathic ASD dataset	3
Idiopathic schizophrenia	3
Idiopathic ADHD	4
Preprocessing	4
Quality Control	5
Gene expression preparation and analyses	5
<b>Supplemental Results</b>	<b>6</b>
Figure 1: Sensitivity analyses on age distribution in 16p11.2 deletion carriers	6
Figure 2: Mirror effects of gene dosage in 16p11.2 CNV are present at the network level	7
Effect of Schizophrenia on FC	8
Effect of ASD on FC	8
Sensitivity analysis testing the effect of medication on FC alterations in autism	8
Effect of ADHD on FC	9
Sensitivity analysis testing the effect of sex on FC alterations in SZ and ADHD	9
Figure 3a: Seed regions showing significant similarity between 16p11.2 deletion and Schizophrenia	10
Figure 3b: Seed regions showing significant similarity between 22q11.2 deletion and Schizophrenia	12
Figure 3c: Seed regions showing significant similarity between 16p11.2 deletion and Autism	14
Figure 3d: Seed regions showing significant similarity between 22q11.2 deletion and Autism	15
Figure 4 Do the same seed regions contribute to the similarity between either 16p11.2 or 22q11.2 deletions and individuals with SZ and ASD?	16
Figure 5: Regional similarities between the individual FC profiles of subjects with a psychiatric diagnosis and FC-signatures of 16p11.2 and 22q11.2 duplications	17
Figure 6: Similarity between the individual FC profiles of subjects with a psychiatric diagnosis and the FC-signatures of the 16p11.2 and 22q11.2 deletions and duplications	19
Figure 7: Loadings of 22q11.2 and 16p11.2 genes and brain regions on PC1	21
Figure 8: Additional information on motion for each cohort after preprocessing	22
<b>References</b>	<b>23</b>

## Supplemental Material and Methods

### Objectives and methods overview

Aim	Objective	Method
AIM1. Characterize the impact of gene dosage on connectivity for CNVs at the 16p11.2 and 22q11.2 genomic loci	1.1. Describe the effect of gene dosage at the 16p11.2 and 22q11.2 genomic loci on global FC.	Connectome Wide Association Study (CWAS): Linear model contrasting CNV carriers with respective controls.
	1.2 Test if deletions and duplications have mirror effects at the connection level.	
AIM2. Test if FC-signatures of deletions represent dimensions observed in idiopathic ASD, SZ, or ADHD.	2.1 Characterize the effect size of idiopathic Autism, Schizophrenia, and ADHD on FC.	Same as 1.1 CWAS: Linear model contrasting cases of each psychiatric groups with respective controls.
	2.2 Test similarities between whole-brain connectomes of CNVs and idiopathic psychiatric conditions.	Pearson correlation between beta maps obtained from each CWAS (case-control contrast) and individual connectomes of either cases or controls of each group.
	2.3 Investigate regions that contribute to similarities observed in 2.2	The same method used in 2.2 applied to each of the 64 regional FC patterns.
	2.4 Identify the relationship between regions identified in 2.3 and cognition	Pearson R computed in 2.3 was correlated to the cognitive measure of each individual
	2.5 Compare the co-expression anatomical patterns of genes within the 16p11.2 CNV and the 22q11.2 CNV	Co-expression matrices for each CNV were obtained by correlating normalized expression values of 22 + 35 genes across 34 brain regions.

## Samples

### 16p11.2 cohort

Imaging data of 16p11.2 CNV carriers and typically developing controls were acquired by the Simons variation in individuals project (VIP) consortium <sup>1</sup> across 2 sites. We excluded 44 individuals from the analysis due to insufficient quality of the imaging data (cf. Supplementary Methods, quality control). The final 16p11.2 sample includes 122 individuals. Over 90% of the deletion carriers and 69% of the duplication carriers met criteria for at least one clinical psychiatric diagnosis (Table 1). Control subjects were recruited from the general population (extra-familial subjects), and had no major DSM-V diagnosis. The duplication group includes 2 individuals with a triplication.

### 22q11.2 cohort

Imaging data of 22q11.2 CNV carriers and typically developing (TD) controls were acquired at the University of California, Los Angeles (UCLA). Patients were ascertained from the UCLA or Children's Hospital, Los Angeles Pediatric Genetics, Allergy/Immunology and/or Craniofacial Clinics. We excluded 16 individuals from the analysis due to insufficient quality of the imaging data (cf. Supplementary Methods, quality control). The final 22q11.2 sample includes 101 individuals. Demographically comparable TD comparison subjects were recruited from the same communities as patients via web-based advertisements and by posting flyers and brochures at local schools, pediatric clinics, and other community sites. Exclusion criteria for all study participants included significant neurological or medical conditions (unrelated to 22q11.2 mutation) that might affect brain structure, history of head injury with loss of consciousness, insufficient fluency in English, and/or substance or alcohol abuse or dependence within the past 6 months. The UCLA Institutional Review Board approved all study procedures and informed consent documents. Scanning was conducted on an identical 3 tesla Siemens Trio MRI scanner with a 12-channel head coil at the University of California at Los Angeles Brain Mapping Center or at the Center for Cognitive Neuroscience <sup>2</sup>.

## Idiopathic ASD dataset

The ABIDE dataset<sup>3</sup> is an aggregate sample of different studies including imaging and behavioural data for individuals with an ASD diagnosis and typically developing peers matched for age. Due to the small number of females in the ABIDE dataset, we excluded female individuals. To better account for biases in connectivity estimation due to differences in recording sites, subject age, and in scanner motion, we created age and motion-matched subsamples for each recording site in ABIDE of individuals that passed our quality control criteria. We then excluded recording sites with fewer than 20 individuals (10 ASD, 10 controls). Our final ABIDE sample thus includes 459 male individuals, 225 individuals with ASD and 234 healthy controls, from 10 recording sites.

## Idiopathic schizophrenia

We used fMRI data retrospectively aggregated from 10 distinct sites and studies. Brain imaging multi-state data were obtained through either the SchizConnect and OpenfMRI data sharing platforms (<http://schizconnect.org><sup>4</sup>; <https://openfmri.org><sup>5</sup>) or local scanning at the University of Montréal. All patients were diagnosed with SZ according to DSM-IV or DSM-V criteria, as a function of the time of study. Sites samples were obtained after subjects were selected in order to ensure even proportions of SZ patients and controls within each site (from N = 9 to N = 42 per group) and to reduce between-group differences with regards to gender ratio (74% vs. 75% males in patients and controls, respectively), age distribution (34 vs. 32 years old on average) and motion levels (averaged frame displacement: 0.16 vs. 0.14 mm). Such matching of SZ and controls subjects was achieved based on propensity scores. In total, we retained 242 SZ patients and 242 healthy controls in statistical analyses. Depending on the study, positive and negative symptoms were assessed with either with the Positive and negative syndrome scale (PANSS,<sup>6</sup>) or the Scales for the assessment of positive/negative symptoms (SAPS/SANS,<sup>7</sup>). In order to allow for group analyses, SAPS/SANS scores were converted into PANSS scores using published regression-based equations<sup>8</sup>.

## Idiopathic ADHD

We used data provided by the ADHD-200 Consortium and The Neuro Bureau ADHD-200 Preprocessed repository (8 cohorts [http://fcon\\_1000.projects.nitrc.org/indi/adhd200/](http://fcon_1000.projects.nitrc.org/indi/adhd200/)<sup>9</sup>). Data from seven sites were retained after exclusion of 184 individuals. We included in our study a total of 763 subjects, 289 patients diagnosed with ADHD and 474 healthy controls.

This database provided child and adolescent data. Scores related to ADHD symptoms were measured using Conner's Parent Rating Scale-Revised, Long Version (CPRS-LV<sup>10</sup>).

## Preprocessing

All datasets were preprocessed using the same parameters with the same Neuroimaging Analysis Kit (NIAK) version 0.12.4, an Octave-based open source processing and analysis pipeline<sup>11</sup>. The first four volumes of each rs-fMRI time series were discarded to allow for magnetization to reach a steady state. Each data set was corrected for differences in slice acquisition time. Head motion parameters were estimated by spatially re-aligning individual timepoints with the median volume in the time series. This reference median volume was then aligned with the individual anatomical T1 image, which in turn was co-registered onto the MNI152 template space using an initial affine transformation, followed by a nonlinear transformation. Finally, each individual timepoint was mapped to the MNI space<sup>12</sup> using the combined spatial transformations. Slow frequency drifts were modeled on the entire time series as discrete cosine basis functions with a 0.01 Hz high-pass cut-off. Timepoints with excessive in-scanner motion (greater than 0.5 mm framewise displacement) were then censored from the time series by removing the affected timepoint as well as the preceding and following two timepoints<sup>13</sup>. Nuisance covariates were regressed from the remaining time series: the previously estimated slow time drifts, the average signals in conservative masks of the white matter and lateral ventricles, and the first principal components (95% energy) of the estimated six rigid-body motion parameters and their squares. Data were then spatially smoothed with a 3D Gaussian kernel (FWHM = 6mm).

## Quality Control

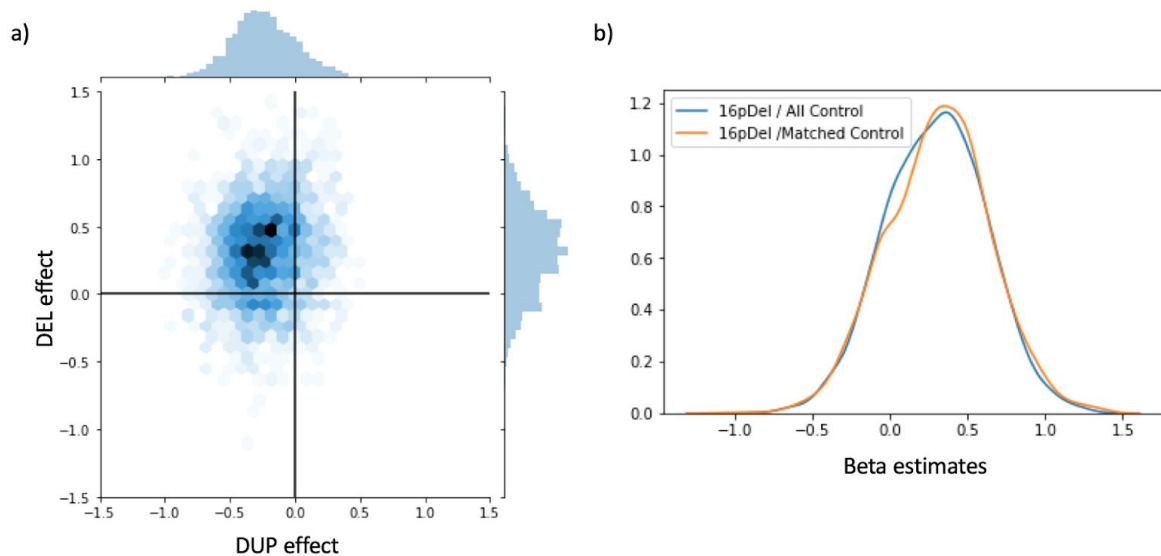
Preprocessed data were visually controlled for quality of the co-registration, head motion, and related artifacts by one rater. Not all six datasets were examined by the same raters, yet all raters followed the same standardized quality-control procedure <sup>14</sup>. If there was co-registration failure of either the functional image to individual T1 or individual T1 to MNI template registration, we attempted a manual fix by changing the parameters of the preprocessing pipeline. Individuals were excluded from the analysis if co-registration errors could not be fixed. Individuals were also excluded from the analysis if the average framewise displacement after motion censoring exceeded 0.5 mm or if fewer than 40 time frames remained (Supplementary Materials and Methods).

## Gene expression preparation and analyses

Gene expression levels were initially computed for each of the 68 cortical regions of the Desikan Atlas, based on the Allen Brain Atlas <sup>15</sup> and accessed April 4th 2017 at [https://figshare.com/articles/A\\_FreeSurfer\\_view\\_of\\_the\\_cortical\\_transcriptome\\_generated\\_from\\_the\\_Allen\\_Human\\_Brain\\_Atlas/1439749](https://figshare.com/articles/A_FreeSurfer_view_of_the_cortical_transcriptome_generated_from_the_Allen_Human_Brain_Atlas/1439749) <sup>16</sup>). Because right hemisphere data were available for only three of the six donor brains, normalization was calculated for each gene by Z-scoring the expression levels across the 34 cortical regions of only the left hemisphere <sup>17</sup> (data available at <http://neanderthal.pasteur.fr>, Supplemental Table S4.1).

## Supplemental Results

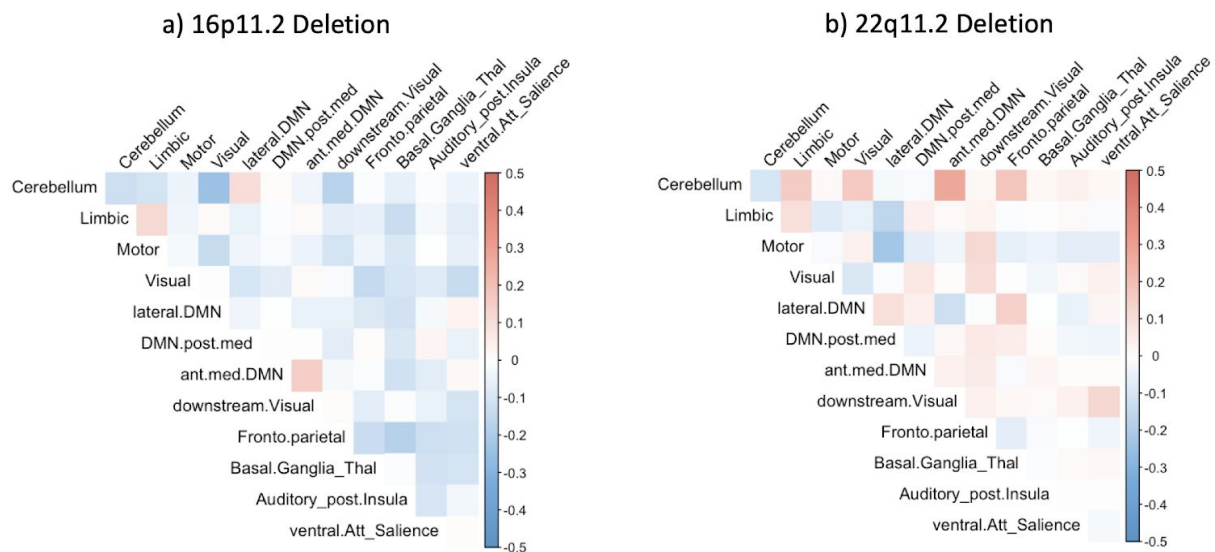
Figure 1: Sensitivity analyses on age distribution in 16p11.2 deletion carriers



Legend: We performed a sensitivity analysis after excluding older controls to obtain identical age distributions (mean 12.7 and 13.0 years respectively) in the 16p11.2 deletions and control groups. The CWAS performed before and after excluding adults provides the same results albeit with decreased power: The 2 beta maps are highly correlated ( $r=0.967$ ) and their distribution (b) overlaps perfectly.

(a): Scatterplot (*hexagonal plot*), showing estimates (beta values) from connectome-wide association studies (CWAS) performed between 16p11.2 CNVs and their respective controls excluding adults to obtain a matched age distribution. The scatterplot is identical to figure 1.a demonstrating that age distribution does not affect our results.

Figure 2: Mirror effects of gene dosage in 16p11.2 CNV are present at the network level



Legend:

We investigated how mirror effects of gene dosage at the individual network level follow the organization of the brain into canonical resting-state networks. Gene dosage effects at the connection level are shown broken down into the 12 corresponding functional brain networks (Supplementary Table S1.10) for the 16p11.2 (a) and 22q11.2 (b) genomic loci. Red colors reflect effects in the same direction for deletions and duplications. Blue colors reflect mirror effects for deletions and duplications (i.e. an increase in FC is associated with one, but a decrease is associated with the other). For the 16p11.2 CNVs, networks exhibited more mirror connectivity alterations than would be expected by chance ( $p = 0.006$ , two-sided). By contrast, 22q11.2 CNVs showed an equal number of connections with mirror and uni-directional alterations across networks.



## Effect of Schizophrenia on FC

Idiopathic SZ showed overall underconnectivity affecting 835 connections, with the strongest alterations affecting the frontoparietal, auditory, ventral attention and limbic networks (dorsal anterior cingulate cortex, dorsal anterior and posterior insula, ventral posterior insula, and inferior marginal sulcus sulcus) (Figures 3a, c, Supplementary Tables S1.7 and S1.9). Over-connectivity was restricted to 24 connections (cerebello-motor and thalamo-auditory), in line with previous reports<sup>18,19</sup> (859 connections survived FDR correction in total,  $q < 0.05$ ,  $p$  ranging from 0.02 to  $1e-12$ ).

## Effect of ASD on FC

Underconnectivity in ASD was driven by seed regions in the limbic, lateral DMN, and cerebellar networks and over-connectivity was observed in the basal ganglia and motor networks, in accordance with previous reports<sup>20</sup> (anterior middle frontal gyrus, temporal pole, anterior middle temporal gyri, lateral fusiform gyrus, and cerebellum VIII-ab) (Figure 3b, c, Supplementary Tables S1.6 and S1.9). Seventy-five connections (73 under and 2 overconnected) survived FDR correction ( $q < 0.05$ ), with  $p$  ranging from 0.01 to  $1e-5$ .

## Sensitivity analysis testing the effect of medication on FC alterations in autism

A sensitivity analysis testing the effect of medication was performed with excluding 55 individuals with autism and one control from the analysis. Connectome-wide analysis on the non-medicated subgroup showed overall underconnectivity. Underconnectivity was significant (FDR) in 28 connections. The beta map of this analysis was highly correlated ( $r = 0.96$ ) with the initial CWAS performed on the full sample including ASD subjects with medication.

## Effect of ADHD on FC

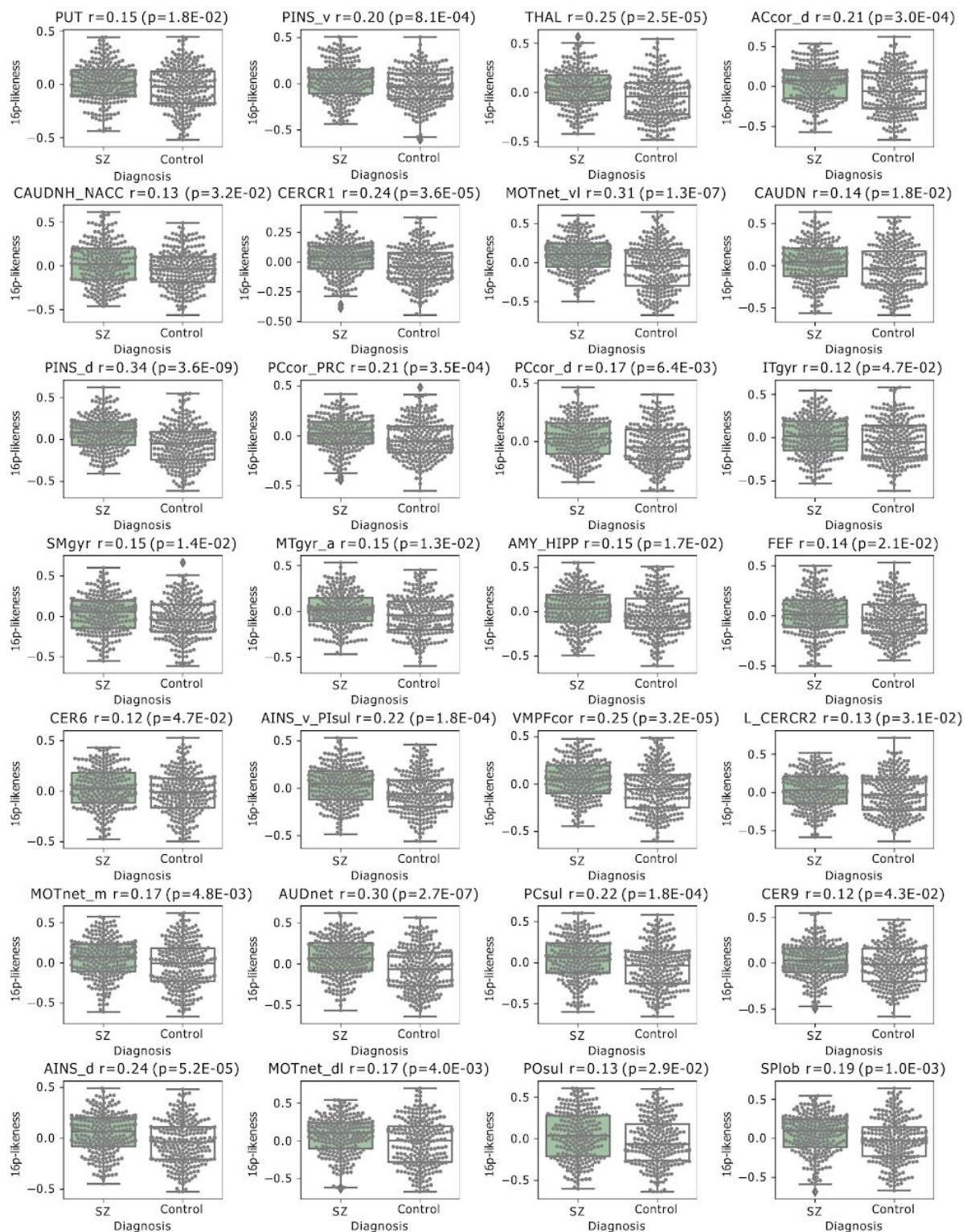
For ADHD, none of the individual connections survived FDR correction (nominally significant alterations were observed in the posterior middle temporal and lateral occipitotemporal gyri, posterior medial visual network, the cerebellum-VI and the left intraparietal sulcus) (Supplementary Tables S1.8 and S1.9).

## Sensitivity analysis testing the effect of sex on FC alterations in SZ and ADHD

A sensitivity analysis was performed on 179 male participants with schizophrenia and 189 male controls. Males with idiopathic SZ also show overall underconnectivity with 472 connections surviving FDR. The beta map of this analysis excluding females was highly correlated ( $r=0.95$ ) with the initial CWAS performed on the full sample.

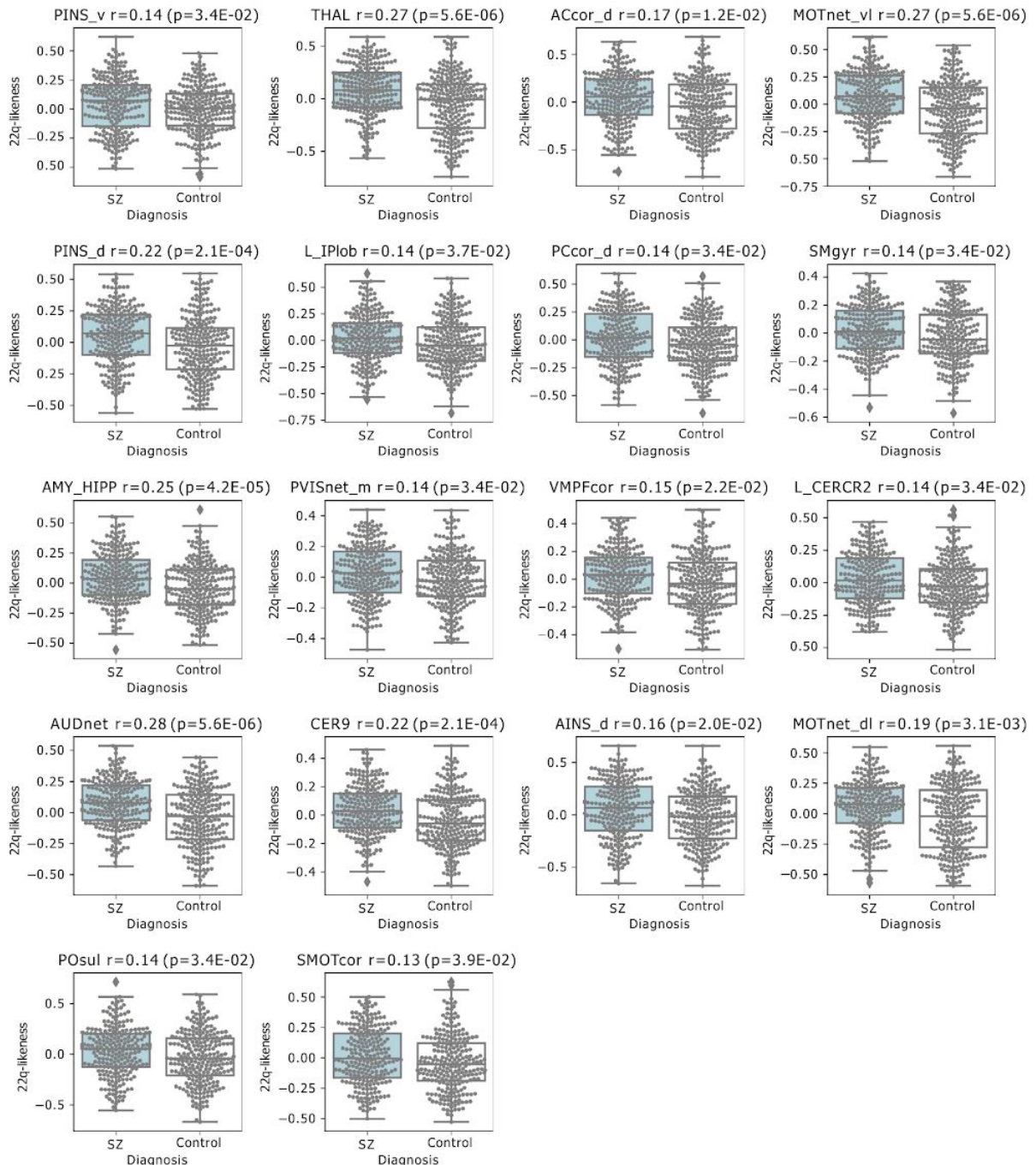
The same analysis was performed in the ADHD sample. The beta map of the analysis excluding females was highly correlated ( $r=0.93$ ) with the initial CWAS performed on the full ADHD sample.

Figure 3a: Seed regions showing significant similarity between 16p11.2 deletion and Schizophrenia



Legend: Similarities between regional FC of 16p11.2 deletions and individuals with idiopathic SZ compared to their respective controls. Grey dots correspond to individuals in either the SZ or control group. Boxplots for individuals with SZ (green) and their respective controls (white) illustrate the observed group differences in similarity values. Similarity values (Pearson's R, Grey dots) were derived by computing Pearson's correlations between the regional FC-signatures. Differences between SZ or controls are tested using a Mann-Whitney U test. We reported significant group differences after FDR correction accounting for the 64 regions ( $q < 0.05$ ).

Figure 3b: Seed regions showing significant similarity between 22q11.2 deletion and Schizophrenia

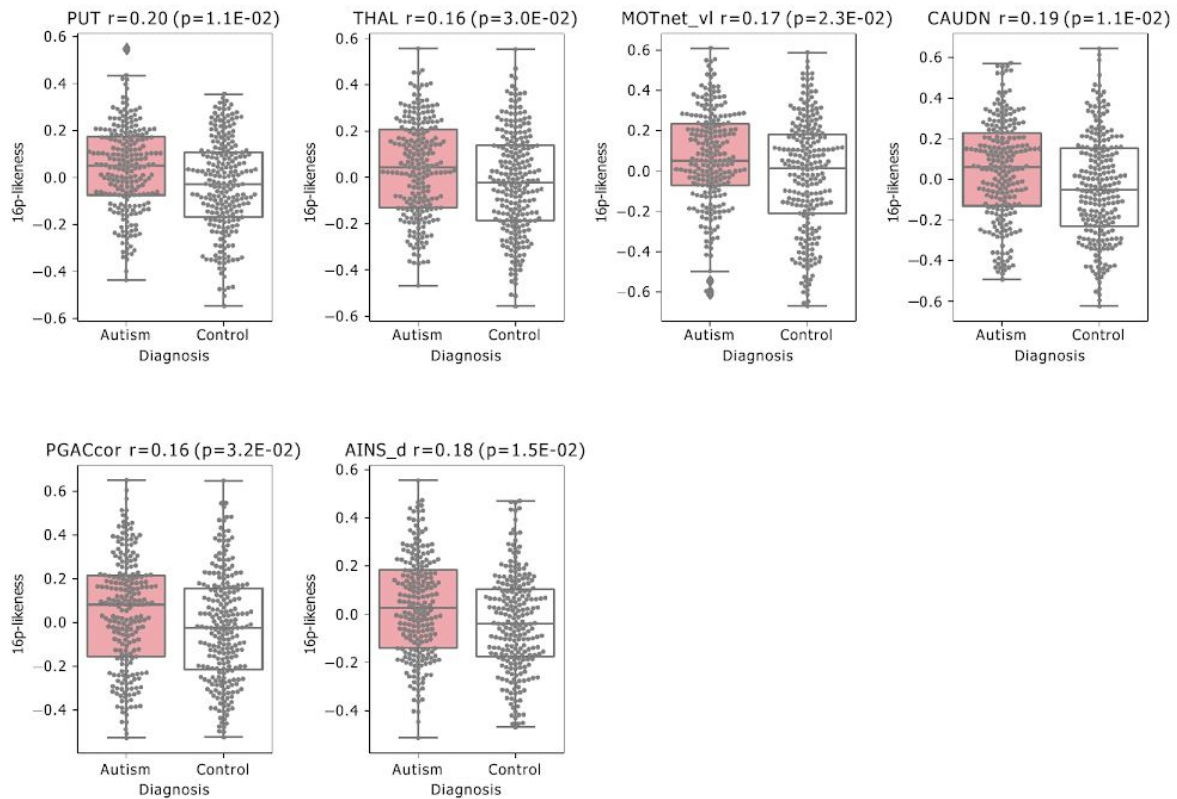


Legend: Similarities between regional FC of 22q11.2 deletions and individuals with SZ compared to controls. Grey dots correspond to individuals in either the SZ or control group. Box plots for

individuals with SZ (blue) and their respective controls (white) illustrate the observed group differences in similarity values.

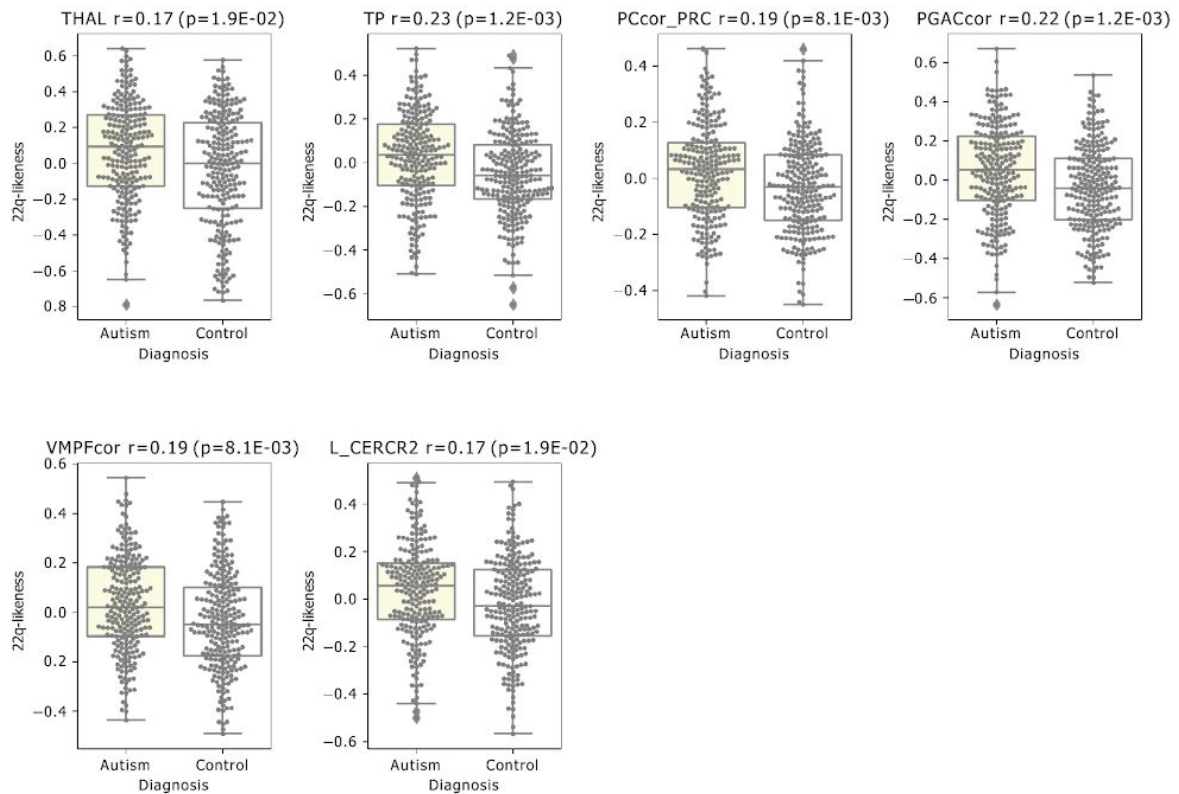
Similarity values (Pearson's R, Grey dots) were derived by computing Pearson's correlations between the regional FC-signatures. Differences between SZ or controls are tested using a Mann-Whitney U test. We reported significant group differences after FDR correction accounting for the 64 regions ( $q < 0.05$ ).

Figure 3c: Seed regions showing significant similarity between 16p11.2 deletion and Autism



Legend: Similarities between regional FC of 16p11.2 deletions and individuals with ASD compared to controls are shown. Grey dots correspond to individuals in either the ASD or control group. Box plots for individuals with ASD (red) and their respective controls (white) illustrate the observed group differences in similarity values. Similarity values (Pearson's R, Grey dots) were derived by computing Pearson's correlations between the regional FC-signatures. Differences between SZ or controls are tested using a Mann-Whitney U test. We reported significant group differences after FDR correction accounting for the 64 regions ( $q < 0.05$ ).

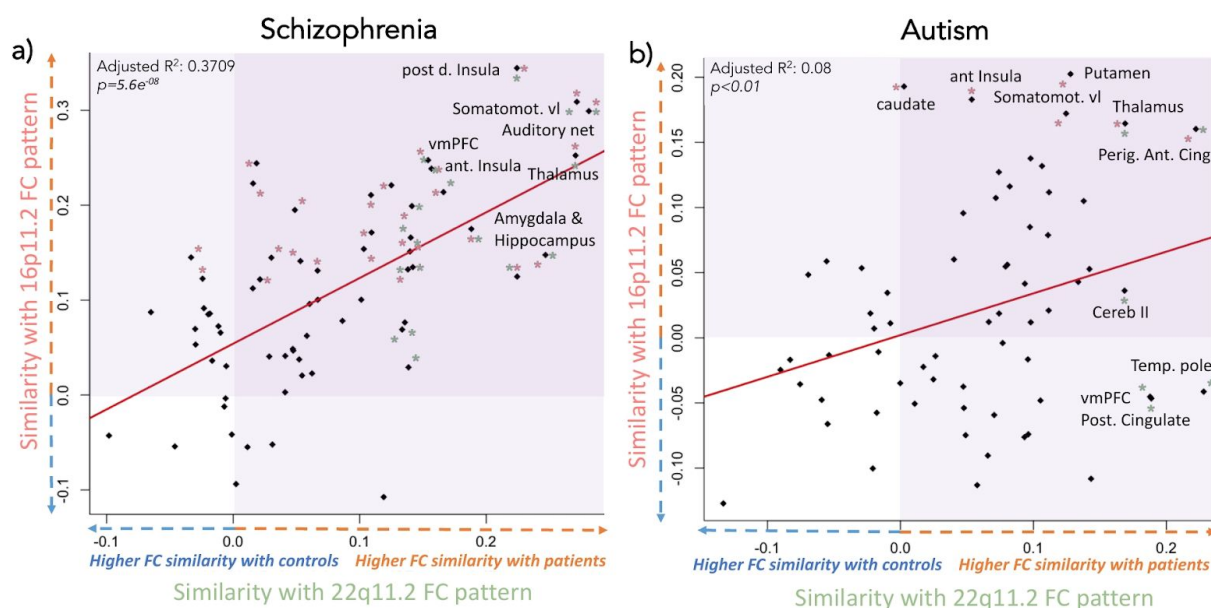
Figure 3d: Seed regions showing significant similarity between 22q11.2 deletion and Autism



Legend: Similarities between regional FC of 22q11.2 deletions and individuals with ASD compared to controls are shown. Grey dots correspond to individuals in either the ASD or control group. Box plots for individuals with ASD (yellow) and their respective controls (white) illustrate the observed group differences in similarity values. Similarity values (Pearson's R, Grey dots) were derived by computing Pearson's correlations between the regional FC-signatures. Differences between SZ or controls are tested using a Mann-Whitney U test. We reported significant group differences after FDR correction accounting for the 64 regions ( $q < 0.05$ ).



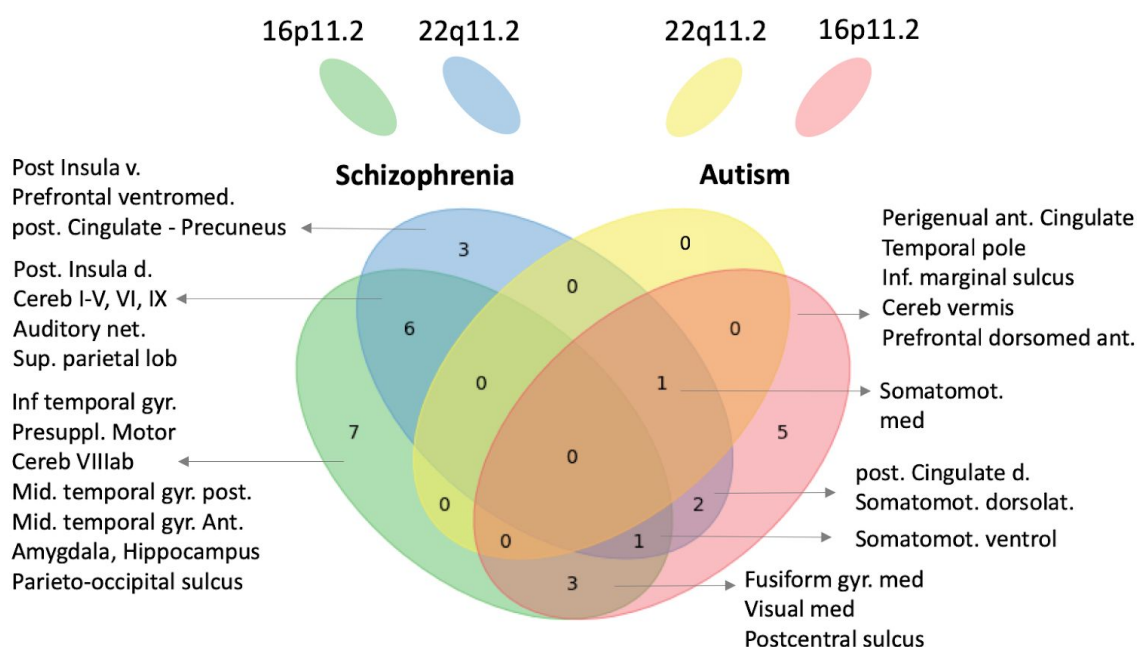
Figure 4 Do the same seed regions contribute to the similarity between either 16p11.2 or 22q11.2 deletions and individuals with SZ and ASD?



Legend: Many of the same seed regions contribute to the similarity between either 16p11.2 or 22q11.2 deletions and individuals with SZ (a). This is less the case for autism.

The horizontal axes show the Mann whitney effect size (rank biserial correlation) representing the connectivity similarity between the 22q11.2 deletion FC-signature and individuals with idiopathic SZ (a) or ASD (b) compared to controls. The vertical axes show values (biserial correlation) representing the connectivity similarity with the 16p11.2 deletion FC-signature and individuals with idiopathic ASD (a) or SZ (b) compared to controls. Positive values (orange arrows) on the horizontal and vertical axes represent higher connectivity similarity between the deletion FC-signatures and individuals with SZ (a) or ASD (b) compared to their respective controls. Negative values (blue arrows) represent a higher similarity with control individuals. Seed-based connectivity signatures that show significant (FDR corrected) connectivity similarity with deletions are colored (pink stars for 16p11.2 and green stars for 22q11.2).

Figure 5: Regional similarities between the individual FC profiles of subjects with a psychiatric diagnosis and FC-signatures of 16p11.2 and 22q11.2 duplications



Legend: The FC-signatures of both duplications (group level) were decomposed into 64 seed-regions.

Deletion FC-signatures are correlated to the individual connectomes of subjects with either ASD, SZ or control subjects. Of note, the correlation results in the mean centering of all region-based FC-signatures. Significantly increased similarities with either ASD and SZ are presented on the right and the left side of the diagram, respectively.

Some of these regions overlap with those identified in the same analysis using FC-signatures of both deletions: SZ individuals show similarities with both 16p11.2 deletion and duplication for 2 regions (Inferior and middle temporal gyrus)

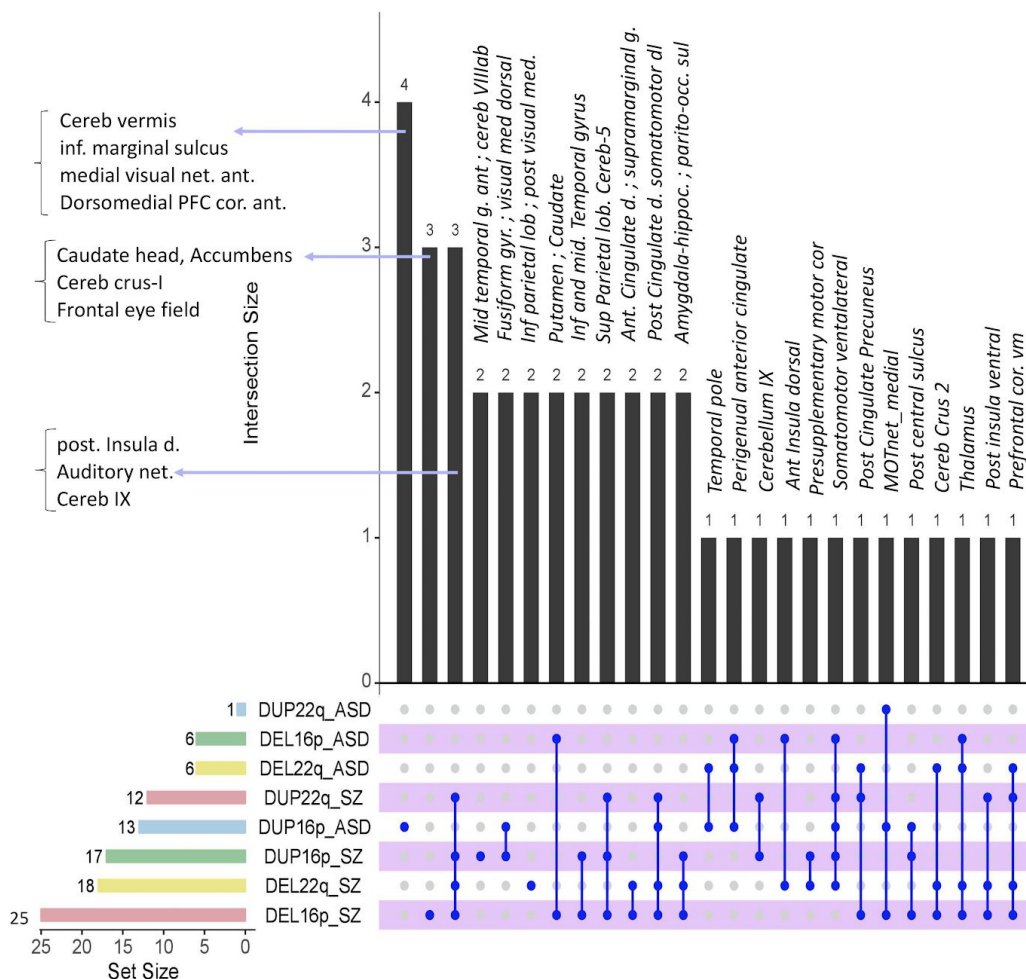
SZ individuals show similarities with both 22q11.2 duplication and deletion for 6 regions (ventral / dorsal posterior insula, ventromedial prefrontal cortex, dorsolateral somatomotor cortex, cerebellum IX, auditory network) and with 16p11.2 duplication and deletions for 9 regions (parieto occipital

*Neuropsychiatric mutations delineate FC dimensions contributing to autism and schizophrenia*

sulcus, amygdala/ hippocampus, inf & middle gyrus anterior and posterior temporal gyrus, superior parietal lobule, cerebellum VI, posterior insula, dorsal prefrontal ventro medial cortex). ASD individuals show similarities with both 16p11.2 deletion and duplication for 2 regions perigenual anterior cingulate cortex, ventrolateral somatomotor cortex.

For 11 regions, controls rather than individuals with ASD or SZ showed increased similarities with duplications. This increased similarity with controls was never observed for deletion FC-signatures.

Figure 6: Similarity between the individual FC profiles of subjects with a psychiatric diagnosis and the FC-signatures of the 16p11.2 and 22q11.2 deletions and duplications



Legend: Because a Venn diagram showing overlapping brain regions across 8 comparisons (conditions, dels and dups) is impractical, we used the UpSet R package<sup>21</sup> to combine results from both Venn-Diagram (presented in Figure 4 (deletion) and in Supplementary Figure 6 (duplication)).

The dark blue lines and points show regions contributing to several similarities.

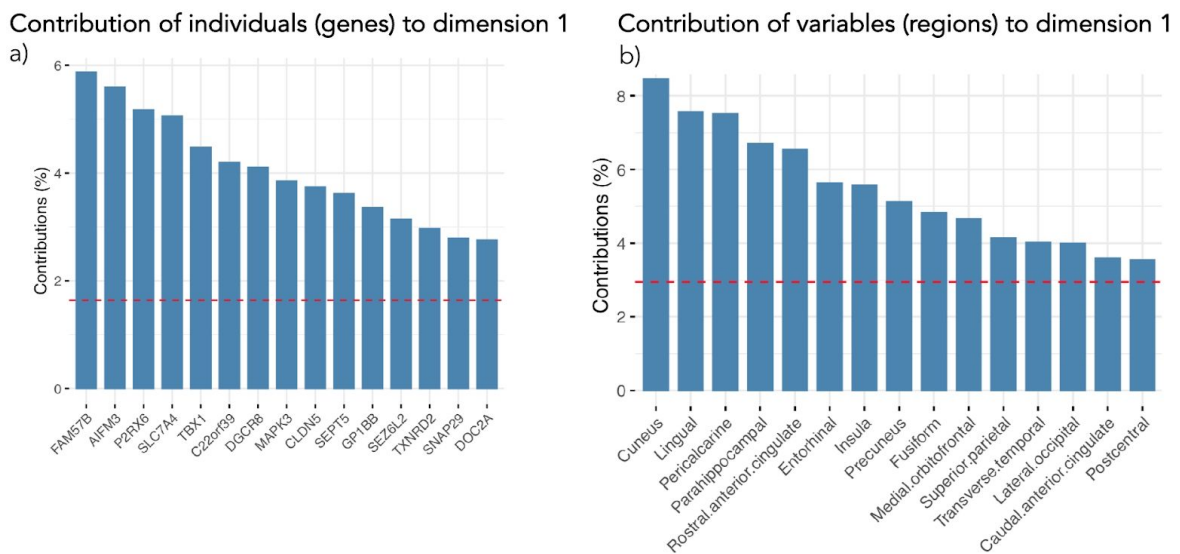
The 8 rows represent the 8 comparisons between the 4 CNVs and idiopathic ASD or SZ.

*Neuropsychiatric mutations delineate FC dimensions contributing to autism and schizophrenia*

For example, the 23rd vertical black bar represents the thalamus which contributes to similarities across 4 comparisons (the 4 connected dark blue dots, representing the 16p11.2 and 22q11.2 deletion-FC-similarity with either ASD or SZ).

Horizontal bars on the bottom left represent the number of seed regions showing significant similarities for each comparison (eg. 6 regions showed similarity between 16p11.2 deletion-FC-signatures and ASD-FC-profiles). Y axis: number of regions showing similarities between CNV carriers and idiopathic SZ or ASD.

Figure 7: Loadings of 22q11.2 and 16p11.2 genes and brain regions on PC1



Legend: Contribution of top genes within 16p11.2 and 22q11.2 loci (a), and top neuroanatomical regions (b) to the first Principal Component. PCA was computed using expression values (individuals) of 57 genes encompassed in both genomic loci across 34 brain regions (variables). We used the R “psych” package<sup>22</sup>.

Figure 8: Additional information on motion for each cohort after preprocessing

	ADHD	CON	SZ	CON	ASD	CON	16PDEL	16PDUP	16PCON	22QDEL	22QDUP	22QCON
Mean (frames)	160	159	152	166	139	153	83	83	85	110	121	126
Sd (frames)	53	59	50	49	52	49	18	23	20	42	34	30
Mean (% scrubbed)	0.13	0.25	*	*	0.24	0.16	0.26	0.25	0.23	0.25	0.18	0.14
Sd (% scrubbed)	0.15	0.26	*	*	0.23	0.18	0.15	0.2	0.16	0.28	0.22	0.2

Mean (frames): mean number of frames remaining after scrubbing per individual; Mean (% scrubbed): Mean percentage of frames excluded per individual; SD: Standard Deviation; 16PDEL: 16p11.2 deletion; 16PCON: 16p11.2 control; 16PDUP: 16p11.2 duplication; 22QDEL: 22QCON: 22q11.2 control; 22q11.2 deletion; 22QDUP: 22q11.2 duplication.

## References

1. Simons Vip Consortium. Simons Variation in Individuals Project (Simons VIP): a genetics-first approach to studying autism spectrum and related neurodevelopmental disorders. *Neuron* **73**, 1063–1067 (2012).
2. Lin, A. *et al.* Mapping 22q11.2 Gene Dosage Effects on Brain Morphometry. *J. Neurosci.* **37**, 6183–6199 (2017).
3. Di Martino, A. *et al.* The autism brain imaging data exchange: towards a large-scale evaluation of the intrinsic brain architecture in autism. *Mol. Psychiatry* **19**, 659–667 (2014).
4. Wang, L. *et al.* SchizConnect: Mediating neuroimaging databases on schizophrenia and related disorders for large-scale integration. *Neuroimage* **124**, 1155–1167 (2016).
5. Poldrack, R. A. *et al.* Toward open sharing of task-based fMRI data: the OpenfMRI project. *Front. Neuroinform.* **7**, 12 (2013).
6. Kay, S. R., Fiszbein, A. & Opler, L. A. The positive and negative syndrome scale (PANSS) for schizophrenia. *Schizophr. Bull.* **13**, 261–276 (1987).
7. Andreasen, N. C. The Scale for the Assessment of Negative Symptoms (SANS): conceptual and theoretical foundations. *Br. J. Psychiatry Suppl.* 49–58 (1989). doi:10.1192/S0007125000291496
8. van Erp, T. G. M. *et al.* Converting positive and negative symptom scores between PANSS and SAPS/SANS. *Schizophr. Res.* **152**, 289–294 (2014).
9. ADHD-200 Consortium. The ADHD-200 Consortium: A Model to Advance the Translational Potential of Neuroimaging in Clinical Neuroscience. *Front. Syst. Neurosci.* **6**, 62 (2012).
10. Conners, C. K., Sitarenios, G., Parker, J. D. & Epstein, J. N. The revised Conners' Parent Rating Scale (CPRS-R): factor structure, reliability, and criterion validity. *J. Abnorm. Child Psychol.* **26**, 257–268 (1998).
11. Bellec, P. *et al.* A neuroimaging analysis kit for Matlab and Octave. in *Proceedings of the 17th International Conference on Functional Mapping of the Human Brain* 2735–2746 (2011).



12. Fonov, V. S., Evans, A. C., McKinstry, R. C., Almlri, C. R. & Collins, D. L. Unbiased nonlinear average age-appropriate brain templates from birth to adulthood. *Neuroimage* **47**, S102 (2009).
13. Power, J. D., Barnes, K. A., Snyder, A. Z., Schlaggar, B. L. & Petersen, S. E. Spurious but systematic correlations in functional connectivity MRI networks arise from subject motion. *Neuroimage* **59**, 2142–2154 (2011).
14. Benhajali, Y. & Bellec, P. Quality Control and assessment of the NIAK functional MRI preprocessing pipeline. (2016). doi:10.6084/m9.figshare.4204845.v1
15. Hawrylycz, M. *et al.* Canonical genetic signatures of the adult human brain. *Nat. Neurosci.* **18**, 1832 (2015).
16. French, L. & Paus, T. A FreeSurfer view of the cortical transcriptome generated from the Allen Human Brain Atlas. *Front. Neurosci.* **9**, 323 (2015).
17. Dumas, G., Malesys, S. & Bourgeron, T. Systematic detection of divergent brain proteins in human evolution and their roles in cognition. *bioRxiv* 658658 (2019). doi:10.1101/658658
18. Ferri, J. *et al.* Resting-state thalamic dysconnectivity in schizophrenia and relationships with symptoms. *Psychol. Med.* **48**, 2492–2499 (2018).
19. Giraldo-Chica, M. & Woodward, N. D. Review of thalamocortical resting-state fMRI studies in schizophrenia. *Schizophr. Res.* **180**, 58–63 (2017).
20. Di Martino, A. *et al.* Aberrant striatal functional connectivity in children with autism. *Biol. Psychiatry* **69**, 847–856 (2011).
21. Conway, J. R., Lex, A. & Gehlenborg, N. UpSetR: an R package for the visualization of intersecting sets and their properties. *Bioinformatics* **33**, 2938–2940 (2017).
22. Revelle, W. R. *psych: Procedures for Personality and Psychological Research.* (2017).

















**Table S1.8** Seed regions ranked by the average absolute effect size estimate in each of the 7 CWAS

Region SZ	ASD	ADHD	16pDel	16pDup	22qDel	22qDup	
1	ANTERIOR_C_MIDDLE_TEV	MIDDLE_TEMPORAL_GYRI	FRONTAL_PC	MIDDLE_TEV	TEMPORAL_I	MEDIAL_VISUAL_NETWORK_posterior	
2	POSTERIOR_TEMPORAL_I	left_INTRAPARIETAL_SULC	CAUDATE_NI	left_INTRAP/	PERIGENUAL	CEREBELLUM_I-V	
3	POSTERIOR_MIDDLE_FRC	POSTERIOR_VISUAL_NETV	PUTAMEN	POSTERIOR_	ANTERIOR_II	POSTERIOR_VISUAL_NETWORK_lateral	
4	ANTERIOR_II	CEREBELLUM_CEREBELLUM_VI	MIDDLE_FRC	CEREBELLUM	ANTERIOR_C	FUSIFORM_GYRUS_lateral	
5	INFERIOR_M	FUSIFORM_C	OCCIPITOTEMPORAL_GYRI	ANTERIOR_C	OCCIPITOTEN	AMYGDALA_LATERAL_VISUAL_NETWORK_anterior	
6	PARIETO_OC	right_INFERII	VISUAL_NETWORK_medio	CEREBELLUM	VISUAL_NET	VENTRAL_M	INFERIOR_TEMPORAL_GYRUS
7	SUPRAMARG	DORSOMEDI	FRONTAL_EYE_FIELD	LATERAL_VIS	FRONTAL_EY	INFERIOR_TI	CEREBELLUM_VI
8	MEDIAL_VISI	FRONTAL_PC	AMYGDALA_and_HIPPOCA	VENTROLATE	AMYGDALA_C	CEREBELLUM	ORBITOFRONTAL_CORTEX
9	ANTERIOR_II	PERIGENUAL	MIDDLE_TEMPORAL_GYRI	PERIGENUAL	MIDDLE_TEV	FUSIFORM_C	POSTERIOR_INSULA_dorsal
10	PERIGENUAL	OCCIPITOTEN	SUPRAMARGINAL_GYRUS	left_INTRAP/	SUPRAMARG	CAUDATE_NI	OCCIPITOTEMPORAL_GYRUS_lateral
11	PRE_SUPPLEI	SUPERIOR_F	INFERIOR_TEMPORAL_GYI	OCCIPITOTEN	INFERIOR_TI	DORSOMEDI	AUDITORY_NETWORK
12	right_INTRAF	VISUAL_NET	POSTERIOR_CINGULATE_C	CEREBELLUM	POSTERIOR_SUPERIOR_P	SUPRAMARGINAL_GYRUS	
13	CEREBELLUM	VENTRAL_M	left_INFERIOR_PARIETAL_C	CEREBELLUM	left_INFERIO	MIDDLE_TEN	POSTERIOR_CINGULATE_CORTEX_dorsal
14	DORSOMEDI	CEREBELLUM	POSTERIOR_CINGULATE_C	DORSAL_VIS	POSTERIOR_CEREBELLUM	MIDDLE_TEMPORAL_GYRUS_anterior	
15	POSTCENTR/	AMYGDALA_POSTERIOR_INSULA_dors	SOMATOMO	POSTERIOR_FRONTAL_PC	AMYGDALA_and_HIPPOCAMPUS		
16	MIDDLE_TEN	AUDITORY_h	CAUDATE_NUCLEUS	POSTERIOR_CAUDATE_NI	DORSOMEDI	left_INFERIOR_PARIETAL_LOBULE	
17	TEMPORAL_I	LATERAL_VIS	FUSIFORM_GYRUS_media	VISUAL_NET	FUSIFORM_C	MIDDLE_FRC	FRONTAL_EYE_FIELD
18	CEREBELLUM	CEREBELLUM	CEREBELLUM_VIIB	AUDITORY_h	CEREBELLUM	CEREBELLUM	POSTERIOR_CINGULATE_CORTEX_and_PRECUNEUS
19	INFERIOR_TI	MEDIAL_VISI	SOMATOMOTOR_NETWORKO	MEDIAL_VISI	SOMATOMO	CEREBELLUM	VISUAL_NETWORK_mediodorsal
20	AMYGDALA_POSTERIOR	left_INFERIOR_FRONTAL_	AMYGDALA_left_INFERIO	ORBITOFRONT	MIDDLE_TEMPORAL_GYRUS_posterior		
21	MIDDLE_TEN	right_INTRAF	CEREBELLUM_CRUSI	CEREBELLUM	CEREBELLUM	MEDIAL_VISI	FUSIFORM_GYRUS_medial
22	PRECUNEUS	ANTERIOR_II	CEREBELLUM_CRUSII_righ	FRONTAL_EY	CEREBELLUM	MIDDLE_TEN	CEREBELLUM_VIIB
23	right_INFERII	SOMATOMO	DORSOMEDIAL_PREFRON	right_MIDDLI	DORSOMEDI	POSTERIOR_SOMATOMOTOR_NETWORK	ventrolateral
24	PUTAMEN	PARIETO_OC	TEMPORAL_POLE	SUPRAMARG	TEMPORAL_I	ANTERIOR_II	left_INFERIOR_FRONTAL_SULCUS
25	AUDITORY_h	ANTERIOR_C	CAUDATE_NUCLEUS_HEAT	LATERAL_VIS	CAUDATE_NI	POSTERIOR_CEREBELLUM_CRUSI	
26	POSTERIOR_SUPRAMARG	ANTERIOR_CINGULATE_C	INFERIOR_M	ANTERIOR_C	PRE_SUPPLEI	CEREBELLUM_CRUSII_right	
27	right_INFERII	POSTERIOR_CEREBELLUM_I-V	FUSIFORM_C	CEREBELLUM	SOMATOMO	DORSOMEDIAL_PREFRONTAL_CORTEX_posterior	
28	SUPERIOR_P	THALAMUS_CEREBELLUM_VIIB	POSTCENTR/	CEREBELLUM	CEREBELLUM	TEMPORAL_POLE	
29	CEREBELLUM	MIDDLE_TEV	THALAMUS	ANTERIOR_II	THALAMUS	SOMATOMO	CAUDATE_NUCLEUS_HEAD_and_NUCLEUS_ACCUMBENS
30	left_INFERIO	INFERIOR_M	CEREBELLUM_VERMIS	SUPERIOR_P	CEREBELLUM	VENTROLATE	ANTERIOR_CINGULATE_CORTEX_dorsal
31	SOMATOMO	LATERAL_VIS	POSTERIOR_INSULA_ventr	POSTERIOR_POSTERIOR_SOMATOMO	CEREBELLUM_VIIB		
32	FUSIFORM_C	DORSAL_VISI	right_INFERIOR_PARIETAL	INFERIOR_TI	right_INFERII	LATERAL_VIS	THALAMUS
33	VENTROLATE	SOMATOMO	INFERIOR_MARGINAL_SUI	PARIETO_OC	INFERIOR_M	POSTERIOR_CEREBELLUM_VERMIS	
34	OCCIPITOTEN	ANTERIOR_II	MEDIAL_VISUAL_NETWORK	SOMATOMO	MEDIAL_VISI	LATERAL_VIS	POSTERIOR_INSULA_ventral
35	VISUAL_NET	CEREBELLUM	right_INTRAPARIETAL_SUI	left_INFERIO	right_INTRAF	POSTERIOR_CAUDATE_NUCLEUS	
36	CEREBELLUM	POSTCENTR/	SUPERIOR_PARIETAL_LOB	right_INTRAF	SUPERIOR_P	POSTERIOR_INFERIOR_MARGINAL_SULCUS	
37	VENTRAL_M	SOMATOMO	SUPERIOR_FRONTAL_GYR	CEREBELLUM	SUPERIOR_F	POSTERIOR_POSTERIOR_VISUAL_NETWORK_medial	
38	MIDDLE_FRC	CAUDATE_NI	PRE_SUPPLEMENTARY_M	SOMATOMO	PRE_SUPPLEI	left_INFERIO	right_INFERIOR_PARIETAL_LOBULE
39	FRONTAL_EY	INFERIOR_TI	LATERAL_VISUAL_NETWORKO	DORSOMEDI	LATERAL_VIS	THALAMUS	SUPERIOR_PARIETAL_LOBULE
40	DORSOMEDI	CEREBELLUM	PARIETO_OCCIPITAL_SULC	CEREBELLUM	PARIETO_OC	CAUDATE_NI	SUPERIOR_FRONTAL_GYRUS_anterior
41	THALAMUS	VENTROLATE	DORSAL_VISUAL_STREAM	THALAMUS	DORSAL_VISI	CEREBELLUM	PRE_SUPPLEMENTARY_MOTOR_CORTEX
42	SOMATOMO	left_INFERIO	SOMATOMOTOR_NETWORKO	left_INFERIO	SOMATOMO	CEREBELLUM	LATERAL_VISUAL_NETWORK_posterior
43	SOMATOMO	PUTAMEN	FRONTAL_POLE_lateral	PRECUNEUS	FRONTAL_PC	left_INFERIO	PARIETO_OCCIPITAL_SULCUS
44	DORSAL_VISI	POSTERIOR_right_INFERIOR_FRONTAL	FUSIFORM_C	right_INFERII	INFERIOR_M	DORSAL_VISUAL_STREAM	
45	left_INTRAP/	right_INFERII	MIDDLE_FRONTAL_GYRUS	TEMPORAL_I	MIDDLE_FRC	SUPRAMARG	SOMATOMOTOR_NETWORK_dorsolateral
46	LATERAL_VIS	PRECUNEUS	DORSOMEDIAL_PREFRON	MIDDLE_TEN	DORSOMEDI	FRONTAL_EY	FRONTAL_POLE_lateral
47	ORBITOFRONT	left_INTRAP/	ANTERIOR_INSULA_dorsal	POSTERIOR_	ANTERIOR_II	SUPERIOR_F	right_INFERIOR_FRONTAL_SULCUS
48	CEREBELLUM	POSTERIOR_VENTROLATERAL_PREFRO	MIDDLE_TEN	VENTROLATE	PARIETO_OC	MIDDLE_FRONTAL_GYRUS_anterior	
49	POSTERIOR_ORBITOFRONT	CEREBELLUM_IX	DORSOMEDI	CEREBELLUM	DORSAL_VISI	DORSOMEDIAL_PREFRONTAL_CORTEX_anterior	
50	CAUDATE_NI	POSTERIOR_PERIGENUAL	ANTERIOR_II	PERIGENUAL	right_INFERII	ANTERIOR_INSULA_dorsal	
51	CEREBELLUM	CEREBELLUM	POSTCENTRAL_SULCUS	ORBITOFRONT	POSTCENTR/	right_INTRAF	VENTROLATERAL_PREFRONTAL_CORTEX
52	POSTERIOR_SUPERIOR_P	AUDITORY_NETWORK	right_INFERII	AUDITORY_h	CEREBELLUM	right_INTRAPARIETAL_SULCUS_and_PARS_ORBITALIS	
53	FRONTAL_PC	PRE_SUPPLEI	SOMATOMOTOR_NETWORKO	SUPERIOR_F	SOMATOMO	POSTCENTR/	CEREBELLUM_IX
54	CAUDATE_NI	CEREBELLUM	CEREBELLUM_CRUSII_left	POSTERIOR_CEREBELLUM	AUDITORY_h	POSTCENTRAL_SULCUS	
55	FUSIFORM_C	CAUDATE_NI	POSTERIOR_VISUAL_NETV	VENTRAL_M	POSTERIOR_CEREBELLUM	SOMATOMOTOR_NETWORK_medial	
56	SUPERIOR_F	CEREBELLUM	VENTRAL_MEDIAL_PREFRI	CEREBELLUM	VENTRAL_M	FUSIFORM_C	CEREBELLUM_CRUSII_left
57	CEREBELLUM	DORSOMEDI	ORBITOFRONTAL_CORTEX	MEDIAL_VISI	ORBITOFRONT	right_MIDDLI	VENTRAL_MEDIAL_PREFRONTAL_CORTEX
58	MEDIAL_VISI	left_INFERIO	FUSIFORM_GYRUS_latera	POSTERIOR_FUSIFORM_C	PRECUNEUS	right_MIDDLE_FRONTAL_GYRUS_posterior	
59	left_INFERIO	CEREBELLUM	right_MIDDLE_FRONTAL_C	CAUDATE_NI	right_MIDDLI	MEDIAL_VISI	PRECUNEUS_dorsal
60	right_MIDDLI	FUSIFORM_C	LATERAL_VISUAL_NETWORKO	right_INFERII	LATERAL_VISI	left_INTRAP/	ANTERIOR_INSULA_ventral_and_PERI_INSULAR_SULCUS
61	LATERAL_VIS	right_MIDDLI	PRECUNEUS_dorsal	PRE_SUPPLEI	PRECUNEUS	right_INFERII	MEDIAL_VISUAL_NETWORK_anterior
62	POSTERIOR_POSTERIOR_	ANTERIOR_INSULA_ventra	CEREBELLUM	ANTERIOR_II	OCCIPITOTEN	PERIGENUAL	ANTERIOR_CINGULATE_CORTEX
63	CEREBELLUM	FRONTAL_EY	MEDIAL_VISUAL_NETWORKO	CEREBELLUM	MEDIAL_VISI	VISUAL_NET	left_INTRAPARIETAL_SULCUS_and_MIDDLE_FRONTAL_GYRUS_posterior
64	CEREBELLUM	MEDIAL_VISI	PUTAMEN	POSTERIOR_PUTAMEN	PUTAMEN	PUTAMEN	PUTAMEN

Table S1.9 Region name and abbreviation legend

ROI_label_64	ROI_full_name_64	Networks_12
PUT	PUTAMEN	BASAL_GANGLIA_and_THALAMUS
PINS_v	POSTERIOR_INSULA_ventral	AUDITORY_NETWORK_and_POSTERIOR_INSULA
CERVM	CEREBELLUM_VERMIS	MESOLIMBIC_NETWORK
THAL	THALAMUS	BASAL_GANGLIA_and_THALAMUS
CER7ab	CEREBELLUM_VIlab	CEREBELLUM
CER5	CEREBELLUM_I-V	CEREBELLUM
ACor_d	ANTERIOR_CINGULATE_CORTEX_dorsal	VENTRAL_ATTENTION_NETWORK_and_SALIENCE_NETWORK
CAUDNH_NACC	CAUDATE_NUCLEUS_HEAD_and_NUCLEUS_ACCUMBENS	MESOLIMBIC_NETWORK
TP	TEMPORAL_POLE	MESOLIMBIC_NETWORK
DMPFcor_p	DORSOMEDIAL_PREFRONTAL_CORTEX	VENTRAL_ATTENTION_NETWORK_and_SALIENCE_NETWORK
R_CERCER2	CEREBELLUM_CRUSII_right	CEREBELLUM
CERCER1	CEREBELLUM_CRUSI	CEREBELLUM
L_IFsul	left_INFERIOR_FRONTAL_SULCUS	FRONTO_PARIETAL_NETWORK
MOTnet_vl	SOMATOMOTOR_NETWORK_ventrolateral	SOMATOMOTOR_NETWORK
CER7b	CEREBELLUM_VIib	CEREBELLUM
FUSgyr_m	FUSIFORM_GYRUS_medial	VENTRAL_VISUAL_STREAM_and_DORSAL_VISUAL_STREAM
CAUDN	CAUDATE_NUCLEUS	BASAL_GANGLIA_and_THALAMUS
PINS_d	POSTERIOR_INSULA_dorsal	AUDITORY_NETWORK_and_POSTERIOR_INSULA
PCor_PRC	POSTERIOR_CINGULATE_CORTEX_and_LOBULE	DEFAULT_MODE_NETWORK_posteromedial
L_IPlob	left_INFERIOR_PARIETAL_LOBULE	DEFAULT_MODE_NETWORK_anteromedial_and_left_ANGULAR_GYRUS
PCor_d	POSTERIOR_CINGULATE_CORTEX_dorsal	VENTRAL_ATTENTION_NETWORK_and_SALIENCE_NETWORK
ITgyr	INFERIOR_TEMPORAL_GYRUS	MESOLIMBIC_NETWORK
SMgyr	SUPRAMARGINAL_GYRUS	VENTRAL_ATTENTION_NETWORK_and_SALIENCE_NETWORK
MTgyr_a	MIDDLE_TEMPORAL_GYRUS_anterior	DEFAULT_MODE_NETWORK_lateral
AMY_HIPP	AMYGDALA_and_HIPPOCAMPUS	MESOLIMBIC_NETWORK
FEF	FRONTAL_EYE_FIELD	VENTRAL_ATTENTION_NETWORK_and_SALIENCE_NETWORK
VISnet_md	VISUAL_NETWORK_mediodorsal	VISUAL_NETWORK
OCCTgyr_l	OCCIPITOTEMPORAL_GYRUS_lateral	VENTRAL_VISUAL_STREAM_and_DORSAL_VISUAL_STREAM
CER6	CEREBELLUM_VI	CEREBELLUM
PVISnet_m	POSTERIOR_VISUAL_NETWORK_medial	VISUAL_NETWORK
R_IPlob	right_INFERIOR_PARIETAL_LOBULE	FRONTO_PARIETAL_NETWORK
IMSul	INFERIOR_MARGINAL_SULCUS	VENTRAL_ATTENTION_NETWORK_and_SALIENCE_NETWORK
MVISnet_p	MEDIAL_VISUAL_NETWORK_posterior	VISUAL_NETWORK
PGACcor	PERIGENUAL_ANTERIOR_CINGULATE_CORTEX	DEFAULT_MODE_NETWORK_anteromedial_and_left_ANGULAR_GYRUS
MVISnet_a	MEDIAL_VISUAL_NETWORK_anterior	VISUAL_NETWORK
AINS_v_Psul	ANTERIOR_INSULA_ventral_and_PERIINSULA	MESOLIMBIC_NETWORK
PRC_d	PRECUNEUS_dorsal	VENTRAL_VISUAL_STREAM_and_DORSAL_VISUAL_STREAM
LVISnet_a	LATERAL_VISUAL_NETWORK_anterior	VISUAL_NETWORK
R_MFgyr_p	right_MIDDLE_FRONTAL_GYRUS_posterior	FRONTO_PARIETAL_NETWORK
FUSgyr_l	FUSIFORM_GYRUS_lateral	VENTRAL_VISUAL_STREAM_and_DORSAL_VISUAL_STREAM
ORBcor	ORBITOFRONTAL_CORTEX	MESOLIMBIC_NETWORK
VMPFcor	VENTRAL_MEDIAL_PREFRONTAL_CORTEX	DEFAULT_MODE_NETWORK_anteromedial_and_left_ANGULAR_GYRUS
PVISnet_l	POSTERIOR_VISUAL_NETWORK_lateral	VISUAL_NETWORK
L_CERCER2	CEREBELLUM_CRUSII_left	CEREBELLUM
MOTnet_m	SOMATOMOTOR_NETWORK_medial	SOMATOMOTOR_NETWORK
AUDnet	AUDITORY_NETWORK	AUDITORY_NETWORK_and_POSTERIOR_INSULA
PCsul	POSTCENTRAL_SULCUS	VENTRAL_ATTENTION_NETWORK_and_SALIENCE_NETWORK
CER9	CEREBELLUM_IX	CEREBELLUM
R_IPsul_PORB	right_INTRAPARIETAL_SULCUS_and_PARIETAL_POLE	FRONTO_PARIETAL_NETWORK
VLPFcor	VENTROLATERAL_PREFRONTAL_CORTEX	DEFAULT_MODE_NETWORK_lateral
AINS_d	ANTERIOR_INSULA_dorsal	VENTRAL_ATTENTION_NETWORK_and_SALIENCE_NETWORK
DMPFcor_a	DORSOMEDIAL_PREFRONTAL_CORTEX	DEFAULT_MODE_NETWORK_anteromedial_and_left_ANGULAR_GYRUS
MFgyr_a	MIDDLE_FRONTAL_GYRUS_anterior	VENTRAL_ATTENTION_NETWORK_and_SALIENCE_NETWORK
R_IFsul	right_INFERIOR_FRONTAL_SULCUS	FRONTO_PARIETAL_NETWORK
FP_l	FRONTAL_POLE_lateral	FRONTO_PARIETAL_NETWORK
MOTnet_dl	SOMATOMOTOR_NETWORK_dorsolateral	SOMATOMOTOR_NETWORK
DVIS	DORSAL_VISUAL_STREAM	VENTRAL_VISUAL_STREAM_and_DORSAL_VISUAL_STREAM
POSul	PARIETO_OCCIPITAL_SULCUS	DEFAULT_MODE_NETWORK_posteromedial
LVISnet_p	LATERAL_VISUAL_NETWORK_posterior	VISUAL_NETWORK
SMOTcor	PRE_SUPPLEMENTARY_MOTOR_CORTEX	VENTRAL_ATTENTION_NETWORK_and_SALIENCE_NETWORK
L_SFgyr_a	left_SUPERIOR_FRONTAL_GYRUS_anterior	DEFAULT_MODE_NETWORK_anteromedial_and_left_ANGULAR_GYRUS
SPlob	SUPERIOR_PARIETAL_LOBULE	SOMATOMOTOR_NETWORK
L_IPsul_MFgyr_p	left_INTRAPARIETAL_SULCUS_and_MIDDLE_FRONTAL_GYRUS	FRONTO_PARIETAL_NETWORK
MTgyr_p	MIDDLE_TEMPORAL_GYRUS_posterior	DEFAULT_MODE_NETWORK_lateral

**Table S2.1** Difference in individual similarity with 16p11.2 deletion FC-signature in individuals with idiopathic autism and controls

U	p_value	median_Autism	median_Control	rank_biserial_correlation	q_value	node_name
20996	0,0002	0,0525	-0,0282		0,2024	0,0113 putamen
24917	0,3218	0,0101	0,0058		0,0535	0,6181 post. insula v.
25832	0,7288	0,0153	0,0139		0,0187	0,8651 cereb vermis
21996	0,0023	0,0436	-0,0217		0,1644	0,0296 thalamus
24376	0,1702	-0,0052	0,0007		-0,0740	0,4539 cereb viiiab
25737	0,6792	0,0129	0,0293		-0,0223	0,8523 cereb i-v
23807	0,0764	0,0250	-0,0164		0,0957	0,2716 ant. cingulate ctx d.
26219	0,9408	0,0082	-0,0119		-0,0040	0,9408 caudate nucleus head, nucleus accumbens
25237	0,4440	-0,0079	-0,0095		-0,0413	0,6608 temporal pole
25955	0,7948	0,0127	0,0007		-0,0141	0,8678 dorsomedial PFC ctx post.
24251	0,1444	0,0345	-0,0294		0,0788	0,4401 cereb crus-II R
26005	0,8221	-0,0095	-0,0060		0,0122	0,8678 cereb crus-I
24810	0,2864	-0,0285	0,0114		-0,0575	0,6181 L inf. frontal sulcus
21795	0,0014	0,0514	0,0141		0,1721	0,0229 somatomot. net. ventrolat.
23945	0,0939	-0,0234	0,0323		-0,0904	0,3165 cereb viib
24780	0,2770	-0,0051	0,0049		0,0587	0,6181 fusiform gyr. medial
21248	0,0004	0,0615	-0,0522		0,1929	0,0113 caudate nucleus
23267	0,0314	0,0374	-0,0041		0,1162	0,1826 post. insula d.
25135	0,4024	-0,0143	-0,0019		-0,0452	0,6439 post. cingulate ctx, precuneus
26138	0,8956	0,0053	-0,0053		0,0071	0,9098 L inf. parietal lobule
23562	0,0518	0,0164	-0,0130		0,1050	0,2073 post. cingulate ctx d.
23348	0,0362	-0,0430	0,0134		-0,1131	0,1897 inf. temporal gyr.
25408	0,5188	0,0014	0,0053		-0,0348	0,6973 supramarginal gyr.
24849	0,2990	0,0021	-0,0088		0,0561	0,6181 mid. temporal gyr. ant.
25889	0,7592	-0,0044	0,0241		-0,0166	0,8676 amygdala, hippocampus
23685	0,0632	-0,0089	0,0194		-0,1003	0,2378 frontal eye field
25387	0,5093	-0,0043	0,0235		-0,0356	0,6973 visual net. mediod.
24318	0,1578	-0,0182	-0,0174		-0,0762	0,4539 occipitotemporal gyr. lat.
25196	0,4270	-0,0031	-0,0096		0,0429	0,6608 cereb vi
25485	0,5546	-0,0010	0,0008		-0,0319	0,7243 post. visual net. medial
23500	0,0468	0,0283	-0,0068		0,1073	0,1996 R inf. parietal lobule
25071	0,3776	-0,0062	0,0131		-0,0476	0,6359 inf. marginal sulcus
25881	0,7549	-0,0104	-0,0034		-0,0169	0,8676 medial visual net. post.
22107	0,0030	0,0817	-0,0241		0,1602	0,0319 perigenual ant. cingulate ctx
25417	0,5230	0,0047	0,0055		0,0345	0,6973 medial visual net. ant.
24765	0,2723	-0,0192	0,0118		-0,0593	0,6181 ant. insula v., peri insular sulcus
25974	0,8051	0,0048	0,0052		-0,0133	0,8678 precuneus d.
25051	0,3700	0,0221	0,0032		0,0484	0,6359 lat. visual net. ant.
25232	0,4419	0,0005	-0,0299		0,0415	0,6608 R mid. frontal gyr. post.
26039	0,8407	0,0035	0,0168		-0,0109	0,8678 fusiform gyr. lat.
23477	0,0450	-0,0187	0,0300		-0,1082	0,1996 orbitofrontal ctx
25100	0,3887	-0,0047	-0,0025		-0,0465	0,6379 v. medial PFC ctx
24584	0,2205	-0,0161	0,0385		-0,0661	0,5645 post. visual net. lat.
25373	0,5030	0,0248	0,0056		0,0362	0,6973 cereb crus-II L
23385	0,0385	0,0707	0,0534		0,1117	0,1897 somatomot. net. medial
22855	0,0146	0,0645	0,0016		0,1318	0,1168 auditory net.
25773	0,6979	0,0154	0,0404		0,0210	0,8589 postcentral sulcus
26012	0,8259	0,0027	0,0010		0,0119	0,8678 cereb ix
22978	0,0185	0,0163	-0,0239		0,1271	0,1186 R intraparietal sulcus, pars orbitalis
25834	0,7299	0,0228	0,0031		0,0187	0,8651 ventrolat. PFC ctx
21511	0,0007	0,0278	-0,0397		0,1829	0,0150 ant. insula d.
22701	0,0108	0,0292	-0,0367		0,1377	0,0983 dorsomedial PFC ctx ant.
24936	0,3284	0,0053	0,0062		0,0528	0,6181 mid. frontal gyr. ant.
22979	0,0185	-0,0435	0,0348		-0,1271	0,1186 R inf. frontal sulcus
25058	0,3727	-0,0122	0,0192		-0,0481	0,6359 frontal pole lat.
24088	0,1154	0,0723	0,0464		0,0850	0,3694 somatomot. net. dorsolat.
25676	0,6480	0,0034	0,0393		-0,0247	0,8295 d. visual stream
24357	0,1661	-0,0376	0,0116		-0,0748	0,4539 parieto occipital sulcus
25338	0,4874	0,0050	0,0411		-0,0375	0,6973 lat. visual net. post.
24993	0,3486	-0,0309	0,0119		-0,0506	0,6359 presupplementary mot. ctx
24886	0,3113	0,0118	-0,0244		0,0547	0,6181 sup. frontal gyr. ant.
26032	0,8369	0,0155	0,0257		0,0111	0,8678 sup. parietal lobule
24907	0,3184	0,0081	0,0458		-0,0539	0,6181 L intraparietal sulcus, mid. frontal gyr. post.
24741	0,2650	0,0113	-0,0196		0,0602	0,6181 mid. temporal gyr. post.

**Table S2.2** Difference in individual similarity with 22q11.2 deletion FC-signature in individuals with idiopathic autism and controls

U	p_value	median_Autism	median_Control	rank_biserial_correlation	q_value	node_name
22959	0,0178	0,0758	0,0013		0,1279	0,0951 putamen
25558	0,5895	0,0005	0,0092		-0,0291	0,7398 post. insula v.
25730	0,6756	-0,0089	0,0203		-0,0226	0,8007 cereb vermis
21878	0,0017	0,0936	-0,0005		0,1689	0,0191 thalamus
23794	0,0749	0,0350	-0,0174		0,0961	0,2109 cereb viiiab
25871	0,7496	-0,0052	-0,0036		0,0172	0,8241 cereb i-v
25082	0,3818	0,0112	-0,0059		0,0472	0,4987 ant. cingulate ctx d.
24302	0,1545	0,0327	-0,0105		0,0768	0,3191 caudate nucleus head, nucleus accumbens
20323	0,0000	0,0359	-0,0595		0,2280	0,0012 temporal pole
25631	0,6254	0,0033	-0,0125		0,0264	0,7698 dorsomedial PFC ctx post.
23403	0,0397	0,0268	-0,0261		0,1110	0,1590 cereb crus-II R
24576	0,2184	0,0071	-0,0160		0,0664	0,3667 cereb crus-I
25857	0,7421	-0,0296	0,0033		-0,0178	0,8241 L inf. frontal sulcus
23047	0,0211	0,0505	0,0001		0,1245	0,1036 somatomot. net. ventrolat.
24595	0,2235	0,0058	-0,0168		0,0657	0,3667 cereb viib
24864	0,3039	-0,0327	-0,0030		-0,0555	0,4562 fusiform gyr. medial
26254	0,9604	0,0212	0,0221		0,0027	0,9757 caudate nucleus
24162	0,1280	0,0094	-0,0375		0,0822	0,2925 post. insula d.
21384	0,0005	0,0338	-0,0312		0,1877	0,0081 post. cingulate ctx, precuneus
25805	0,7146	-0,0152	0,0154		-0,0198	0,8167 L inf. parietal lobule
22697	0,0107	0,0276	-0,0239		0,1378	0,0759 post. cingulate ctx d.
24806	0,2851	-0,0064	-0,0072		0,0577	0,4451 inf. temporal gyr.
26321	0,9980	-0,0094	0,0079		-0,0002	0,9980 supramarginal gyr.
24209	0,1365	0,0231	-0,0177		0,0804	0,3012 mid. temporal gyr. ant.
23802	0,0758	0,0235	-0,0129		0,0958	0,2109 amygdala, hippocampus
25779	0,7010	0,0008	-0,0002		-0,0207	0,8157 frontal eye field
24339	0,1622	-0,0282	0,0478		-0,0754	0,3208 visual net. mediod.
23870	0,0840	0,0243	0,0035		0,0933	0,2151 occipitotemporal gyr. lat.
22806	0,0133	0,0221	-0,0021		0,1337	0,0793 cereb vi
25672	0,6460	0,0076	0,0090		0,0248	0,7801 post. visual net. medial
24437	0,1840	0,0190	0,0044		0,0717	0,3364 R inf. parietal lobule
24767	0,2729	-0,0090	0,0126		-0,0592	0,4367 inf. marginal sulcus
24142	0,1245	-0,0301	0,0215		-0,0829	0,2925 medial visual net. post.
20477	0,0000	0,0524	-0,0418		0,2221	0,0012 perigenual ant. cingulate ctx
26067	0,8562	-0,0069	-0,0025		-0,0098	0,8983 medial visual net. ant.
24469	0,1915	0,0224	-0,0173		0,0705	0,3405 ant. insula v., peri insular sulcus
24912	0,3201	0,0039	0,0152		-0,0537	0,4562 precuneus d.
24501	0,1993	-0,0093	0,0181		-0,0693	0,3447 lat. visual net. ant.
23862	0,0830	0,0074	-0,0231		0,0936	0,2151 R mid. frontal gyr. post.
25890	0,7597	-0,0065	0,0082		-0,0165	0,8241 fusiform gyr. lat.
22552	0,0079	0,0401	-0,0158		0,1433	0,0677 orbitofrontal ctx
21360	0,0005	0,0215	-0,0499		0,1886	0,0081 v. medial PFC ctx
24884	0,3106	-0,0229	0,0131		-0,0547	0,4562 post. visual net. lat.
21889	0,0018	0,0566	-0,0294		0,1685	0,0191 cereb crus-II L
23384	0,0385	0,0572	-0,0063		0,1117	0,1590 somatomot. net. medial
23523	0,0486	0,0248	0,0177		0,1064	0,1816 auditory net.
23391	0,0389	0,0425	-0,0021		0,1115	0,1590 postcentral sulcus
23746	0,0695	0,0394	-0,0135		0,0980	0,2109 cereb ix
24377	0,1704	0,0077	-0,0155		0,0740	0,3208 R intraparietal sulcus, pars orbitalis
24373	0,1695	0,0198	-0,0171		0,0742	0,3208 ventrolat. PFC ctx
24914	0,3208	0,0065	-0,0007		0,0536	0,4562 ant. insula d.
23749	0,0698	0,0139	-0,0235		0,0979	0,2109 dorsomedial PFC ctx ant.
22584	0,0085	0,0339	-0,0456		0,1421	0,0677 mid. frontal gyr. ant.
22820	0,0136	-0,0395	0,0281		-0,1331	0,0793 R inf. frontal sulcus
23553	0,0511	0,0172	-0,0074		0,1053	0,1816 frontal pole lat.
23762	0,0713	0,0406	0,0076		0,0974	0,2109 somatomot. net. dorsolat.
23951	0,0948	-0,0340	0,0192		-0,0902	0,2333 d. visual stream
25034	0,3637	0,0097	-0,0084		0,0490	0,4987 parieto occipital sulcus
25080	0,3810	0,0117	-0,0280		0,0473	0,4987 lat. visual net. post.
26042	0,8424	-0,0243	-0,0056		0,0108	0,8983 presupplementary mot. ctx
24244	0,1431	0,0197	-0,0087		0,0791	0,3052 sup. frontal gyr. ant.
26126	0,8889	0,0263	0,0300		-0,0076	0,9176 sup. parietal lobule
25069	0,3768	0,0057	-0,0044		0,0477	0,4987 L intraparietal sulcus, mid. frontal gyr. post.
25265	0,4558	0,0080	0,0060		0,0403	0,5834 mid. temporal gyr. post.

**Table S2.3** Difference in individual similarity with 16p11.2 deletion FC-signature in individuals with idiopathic schizophrenia and controls

U	p_value	median_SZ	median_Control	rank_biserial_correlation	q_value	node_name
25036	0,0058	0,0163	-0,0212		0,1450	0,0180 putamen
23452	0,0002	0,0554	-0,0335		0,1991	0,0008 post. insula v.
28680	0,6958	0,0089	-0,0093		0,0206	0,7300 cereb vermis
21892	0,0000	0,0584	-0,0396		0,2524	0,0000 thalamus
25991	0,0325	0,0232	-0,0178		0,1124	0,0716 cereb viiiab
26994	0,1371	0,0188	-0,0278		0,0781	0,2249 cereb i-v
23022	0,0000	0,0723	-0,0595		0,2138	0,0003 ant. cingulate ctx d.
25444	0,0126	0,0213	-0,0363		0,1311	0,0323 caudate nucleus head, nucleus accumbens
27860	0,3555	-0,0076	-0,0477		0,0486	0,4551 temporal pole
26342	0,0561	0,0284	-0,0394		0,1004	0,1123 dorsomedial PFC ctx post.
26769	0,1024	0,0135	-0,0045		0,0858	0,1772 cereb crus-II R
22133	0,0000	0,0436	-0,0396		0,2441	0,0000 cereb crus-I
27243	0,1852	-0,0082	-0,0185		0,0696	0,2811 L inf. frontal sulcus
20238	0,0000	0,1119	-0,0381		0,3089	0,0000 somatomot. net. ventrolat.
28391	0,5627	0,0174	0,0011		0,0304	0,6209 cereb viib
28076	0,4333	0,0060	-0,0064		0,0412	0,5118 fusiform gyr. medial
25045	0,0059	0,0472	-0,0327		0,1447	0,0180 caudate nucleus
19196	0,0000	0,0863	-0,0483		0,3444	0,0000 post. insula d.
23113	0,0001	0,0271	-0,0521		0,2107	0,0004 post. cingulate ctx, precuneus
27042	0,1455	0,0047	-0,0301		0,0765	0,2328 L inf. parietal lobule
24425	0,0016	0,0254	-0,0457		0,1659	0,0064 post. cingulate ctx d.
25692	0,0196	0,0185	-0,0500		0,1226	0,0466 inf. temporal gyr.
24852	0,0040	0,0548	-0,0433		0,1513	0,0142 supramarginal gyr.
24776	0,0034	0,0174	-0,0401		0,1539	0,0128 mid. temporal gyr. ant.
24960	0,0050	0,0334	-0,0502		0,1476	0,0167 amygdala, hippocampus
25150	0,0072	0,0122	-0,0429		0,1411	0,0211 frontal eye field
28183	0,4752	0,0072	-0,0136		0,0375	0,5431 visual net. mediod.
27724	0,3114	0,0074	-0,0150		0,0532	0,4152 occipitotemporal gyr. lat.
25714	0,0204	0,0237	-0,0118		0,1218	0,0466 cereb vi
28427	0,5786	0,0006	-0,0308		0,0292	0,6276 post. visual net. medial
28222	0,4910	0,0075	-0,0213		0,0362	0,5513 R inf. parietal lobule
28615	0,6649	-0,0126	-0,0071		0,0228	0,7092 inf. marginal sulcus
26604	0,0818	0,0145	-0,0128		0,0915	0,1496 medial visual net. post.
27697	0,3031	-0,0241	0,0007		-0,0541	0,4127 perigenual ant. cingulate ctx
29195	0,9552	0,0203	0,0303		0,0030	0,9552 medial visual net. ant.
22755	0,0000	0,0464	-0,0618		0,2229	0,0002 ant. insula v., peri insular sulcus
28031	0,4163	-0,0097	0,0218		-0,0427	0,5118 precuneus d.
27756	0,3214	-0,0043	0,0385		-0,0521	0,4198 lat. visual net. ant.
27911	0,3730	0,0177	-0,0170		0,0468	0,4681 R mid. frontal gyr. post.
27159	0,1677	0,0368	0,0055		0,0725	0,2618 fusiform gyr. lat.
26343	0,0561	0,0227	-0,0304		0,1004	0,1123 orbitofrontal ctx
22036	0,0000	0,0505	-0,0531		0,2475	0,0000 v. medial PFC ctx
27677	0,2970	-0,0065	0,0185		-0,0548	0,4127 post. visual net. lat.
25407	0,0118	0,0326	-0,0310		0,1323	0,0314 cereb crus-II L
24268	0,0011	0,0730	-0,0056		0,1712	0,0048 somatomot. net. medial
20523	0,0000	0,0738	-0,0632		0,2991	0,0000 auditory net.
22810	0,0000	0,0682	-0,0325		0,2210	0,0002 postcentral sulcus
25628	0,0176	0,0278	-0,0136		0,1248	0,0432 cereb ix
28093	0,4398	0,0346	-0,0130		0,0406	0,5118 R intraparietal sulcus, pars orbitalis
26136	0,0409	0,0089	0,0393		-0,1074	0,0873 ventrolat. PFC ctx
22299	0,0000	0,0685	-0,0367		0,2385	0,0001 ant. insula d.
26537	0,0744	-0,0451	0,0214		-0,0937	0,1401 dorsomedial PFC ctx ant.
27456	0,2354	0,0115	0,0013		0,0624	0,3348 mid. frontal gyr. ant.
26472	0,0678	0,0176	-0,0170		0,0960	0,1315 R inf. frontal sulcus
28065	0,4291	-0,0062	0,0219		-0,0416	0,5118 frontal pole lat.
24158	0,0009	0,1053	0,0026		0,1750	0,0040 somatomot. net. dorsolat.
27358	0,2112	0,0468	-0,0128		0,0657	0,3072 d. visual stream
25336	0,0103	0,0335	-0,0648		0,1348	0,0287 parieto occipital sulcus
26791	0,1055	0,0331	-0,0011		0,0851	0,1777 lat. visual net. post.
27260	0,1889	-0,0121	-0,0303		0,0691	0,2811 presupplementary mot. ctx
29179	0,9469	0,0046	-0,0157		-0,0035	0,9552 sup. frontal gyr. ant.
23573	0,0002	0,0985	-0,0279		0,1950	0,0010 sup. parietal lobule
26726	0,0967	0,0216	-0,0239		0,0873	0,1719 L intraparietal sulcus, mid. frontal gyr. post.
28927	0,8178	0,0026	0,0067		-0,0121	0,8441 mid. temporal gyr. post.

**Table S2.4** Difference in individual similarity with 22q11.2 deletion FC-signature in individuals with idiopathic schizophrenia and controls

U	p_value	median_SZ	media_Control	rank_biserial_correlation	q_value	node_name
28309	0,5273	0,0113	0,0478	-0,0332	0,7970	putamen
25145	0,0072	0,0710	0,0053	0,1413	0,0343	post. insula v.
27687	0,3000	0,0027	-0,0044	0,0545	0,5818	cereb vermis
21358	0,0000	0,0801	-0,0067	0,2706	0,0000	thalamus
28826	0,7672	0,0188	0,0153	0,0156	0,8768	cereb viiiab
26752	0,1001	-0,0064	-0,0247	0,0864	0,2465	cereb i-v
24415	0,0016	0,0562	-0,0445	0,1662	0,0125	ant. cingulate ctx d.
27328	0,2042	0,0166	-0,0182	0,0667	0,4667	caudate nucleus head, nucleus accumbens
27901	0,3696	0,0101	-0,0136	0,0472	0,6224	temporal pole
26317	0,0540	0,0193	-0,0308	0,1013	0,1440	dorsomedial PFC ctx post.
28745	0,7273	-0,0051	0,0009	-0,0183	0,8768	cereb crus-II R
28740	0,7249	-0,0123	-0,0141	0,0185	0,8768	cereb crus-I
28404	0,5684	-0,0152	0,0039	-0,0300	0,7970	L inf. frontal sulcus
21329	0,0000	0,0716	-0,0368	0,2716	0,0000	somatomot. net. ventrolat.
29123	0,9179	0,0119	0,0200	-0,0054	0,9476	cereb viib
28076	0,4333	0,0037	-0,0201	0,0412	0,6782	fusiform gyr. medial
28397	0,5654	0,0105	0,0068	0,0302	0,7970	caudate nucleus
22715	0,0000	0,0723	-0,0248	0,2243	0,0002	post. insula d.
26092	0,0382	0,0269	-0,0250	0,1089	0,1110	post. cingulate ctx, precuneus
25308	0,0098	0,0199	-0,0457	0,1357	0,0369	L inf. parietal lobule
25173	0,0076	0,0186	-0,0427	0,1403	0,0343	post. cingulate ctx d.
28575	0,6461	0,0118	0,0171	-0,0241	0,8614	inf. temporal gyr.
25188	0,0078	0,0109	-0,0448	0,1398	0,0343	supramarginal gyr.
26258	0,0494	0,0214	-0,0338	0,1033	0,1374	mid. temporal gyr. ant.
22054	0,0000	0,0379	-0,0482	0,2468	0,0000	amygdala, hippocampus
27725	0,3117	0,0233	-0,0173	0,0532	0,5860	frontal eye field
27753	0,3205	0,0199	-0,0190	0,0522	0,5860	visual net. mediod.
28414	0,5728	0,0207	0,0226	-0,0296	0,7970	occipitotemporal gyr. lat.
28660	0,6862	-0,0133	-0,0074	0,0212	0,8768	cereb vi
25224	0,0084	0,0262	-0,0236	0,1386	0,0343	post. visual net. medial
28797	0,7528	0,0024	0,0086	-0,0166	0,8768	R inf. parietal lobule
27456	0,2354	0,0082	-0,0005	0,0624	0,5022	inf. marginal sulcus
28606	0,6606	-0,0223	0,0127	-0,0231	0,8628	medial visual net. post.
27934	0,3811	0,0195	0,0235	-0,0460	0,6254	perigenual ant. cingulate ctx
28079	0,4344	-0,0025	-0,0056	0,0411	0,6782	medial visual net. ant.
28821	0,7647	-0,0026	0,0256	0,0157	0,8768	ant. insula v., peri insular sulcus
26409	0,0619	-0,0412	0,0045	-0,0981	0,1584	precuneus d.
28373	0,5548	0,0137	-0,0106	0,0310	0,7970	lat. visual net. ant.
27892	0,3664	0,0038	-0,0005	0,0475	0,6224	R mid. frontal gyr. post.
28942	0,8253	0,0015	-0,0148	-0,0116	0,9152	fusiform gyr. lat.
27323	0,2030	0,0140	0,0013	0,0669	0,4667	orbitofrontal ctx
24770	0,0034	0,0321	-0,0328	0,1541	0,0215	v. medial PFC ctx
28950	0,8294	0,0054	0,0075	0,0113	0,9152	post. visual net. lat.
25238	0,0086	0,0178	-0,0288	0,1381	0,0343	cereb crus-II L
26080	0,0374	0,0356	-0,0027	0,1094	0,1110	somatomot. net. medial
21051	0,0000	0,0779	-0,0302	0,2811	0,0000	auditory net.
25621	0,0173	0,0443	-0,0077	0,1250	0,0584	postcentral sulcus
22710	0,0000	0,0296	-0,0575	0,2244	0,0002	cereb ix
28447	0,5875	0,0138	0,0030	0,0285	0,8000	R intraparietal sulcus, pars orbitalis
25798	0,0236	0,0196	-0,0248	0,1190	0,0754	ventrolat. PFC ctx
24693	0,0029	0,0669	-0,0166	0,1567	0,0203	ant. insula d.
29214	0,9650	0,0032	-0,0011	0,0023	0,9803	dorsomedial PFC ctx ant.
27576	0,2676	0,0191	-0,0080	0,0583	0,5352	mid. frontal gyr. ant.
27512	0,2501	0,0101	-0,0142	0,0604	0,5163	R inf. frontal sulcus
29251	0,9842	-0,0039	0,0094	-0,0011	0,9842	frontal pole lat.
23770	0,0003	0,0782	-0,0217	0,1882	0,0031	somatomot. net. dorsolat.
28990	0,8497	-0,0080	-0,0037	-0,0100	0,9217	d. visual stream
25124	0,0069	0,0529	-0,0436	0,1420	0,0343	parieto occipital sulcus
28707	0,7088	-0,0213	0,0109	-0,0196	0,8768	lat. visual net. post.
25371	0,0110	-0,0067	-0,0534	0,1336	0,0392	presupplementary mot. ctx
29108	0,9102	0,0046	0,0083	-0,0059	0,9476	sup. frontal gyr. ant.
27853	0,3531	0,0389	0,0105	0,0488	0,6224	sup. parietal lobule
27380	0,2165	0,0031	0,0292	-0,0650	0,4777	L intraparietal sulcus, mid. frontal gyr. post.
29078	0,8948	-0,0080	0,0064	-0,0070	0,9476	mid. temporal gyr. post.

**Table S2.5** Difference in individual similarity with 16p11.2 deletion FC-signature in individuals with idiopathic ADHD and controls

U	p_value	median_ADHD	median_Control	rank_biserial_correlation	q_value	node_name
9780	0,7393	-0,0019	0,0189	-0,0230	0,9725	putamen
9893	0,8658	0,0218	0,0185	0,0117	0,9734	post. insula v.
9662	0,6143	-0,0066	0,0081	0,0348	0,9725	cereb vermis
9877	0,8476	0,0350	0,0020	0,0133	0,9734	thalamus
9267	0,2816	0,0284	-0,0133	0,0742	0,9725	cereb viiiab
9862	0,8306	-0,0108	-0,0017	0,0148	0,9734	cereb i-v
9185	0,2318	0,0520	-0,0070	0,0824	0,9725	ant. cingulate ctx d.
9299	0,3028	0,0257	-0,0169	0,0710	0,9725	caudate nucleus head, nucleus accumbens
9850	0,8171	0,0069	-0,0006	0,0160	0,9734	temporal pole
9487	0,4486	0,0181	0,0086	0,0522	0,9725	dorsomedial PFC ctx post.
9914	0,8898	0,0202	0,0314	0,0096	0,9734	cereb crus-II R
9264	0,2796	-0,0182	-0,0042	-0,0745	0,9725	cereb crus-I
9791	0,7513	0,0163	0,0002	0,0219	0,9725	L inf. frontal sulcus
9481	0,4434	0,0444	0,0937	-0,0528	0,9725	somatomot. net. ventrolat.
9274	0,2861	0,0259	0,0148	0,0735	0,9725	cereb viib
9739	0,6948	0,0019	0,0131	-0,0271	0,9725	fusiform gyr. medial
9284	0,2927	-0,0139	-0,0365	0,0725	0,9725	caudate nucleus
9382	0,3628	0,0725	0,0263	0,0627	0,9725	post. insula d.
10003	0,9925	0,0061	0,0148	0,0007	0,9925	post. cingulate ctx, precuneus
9139	0,2068	-0,0224	0,0056	-0,0870	0,9725	L inf. parietal lobule
9818	0,7812	-0,0100	0,0121	-0,0192	0,9725	post. cingulate ctx d.
9147	0,2110	0,0112	-0,0412	0,0862	0,9725	inf. temporal gyr.
8785	0,0758	0,0394	-0,0190	0,1224	0,9725	supramarginal gyr.
9570	0,5239	0,0008	0,0013	0,0440	0,9725	mid. temporal gyr. ant.
9267	0,2816	0,0174	-0,0081	0,0742	0,9725	amygdala, hippocampus
9926	0,9036	-0,0396	0,0142	0,0084	0,9734	frontal eye field
9248	0,2694	0,0194	-0,0309	0,0761	0,9725	visual net. mediod.
9805	0,7668	-0,0010	-0,0058	0,0205	0,9725	occipitotemporal gyr. lat.
9097	0,1857	0,0343	-0,0126	0,0912	0,9725	cereb vi
9080	0,1777	-0,0249	0,0163	-0,0929	0,9725	post. visual net. medial
9664	0,6163	-0,0271	-0,0289	-0,0346	0,9725	R inf. parietal lobule
9182	0,2301	0,0792	-0,0139	0,0827	0,9725	inf. marginal sulcus
8751	0,0680	0,0297	-0,0237	0,1258	0,9725	medial visual net. post.
9809	0,7712	0,0048	-0,0134	0,0201	0,9725	perigenual ant. cingulate ctx
9380	0,3613	0,0182	-0,0229	0,0629	0,9725	medial visual net. ant.
9324	0,3202	0,0162	0,0010	0,0685	0,9725	ant. insula v., peri insular sulcus
9748	0,7045	-0,0080	0,0009	-0,0262	0,9725	precuneus d.
9736	0,6916	0,0144	0,0274	-0,0274	0,9725	lat. visual net. ant.
9316	0,3145	0,0373	0,0155	0,0693	0,9725	R mid. frontal gyr. post.
9533	0,4895	0,0097	0,0276	-0,0477	0,9725	fusiform gyr. lat.
9539	0,4950	0,0204	-0,0088	0,0471	0,9725	orbitofrontal ctx
9971	0,9555	0,0065	-0,0144	0,0039	0,9765	v. medial PFC ctx
9474	0,4374	0,0102	-0,0147	0,0535	0,9725	post. visual net. lat.
9738	0,6938	0,0087	0,0136	-0,0272	0,9725	cereb crus-II L
9976	0,9613	0,0962	0,0216	-0,0034	0,9765	somatomot. net. medial
9674	0,6266	0,0846	0,0640	0,0336	0,9725	auditory net.
9826	0,7901	0,0712	0,0296	-0,0184	0,9725	postcentral sulcus
9734	0,6895	0,0231	-0,0031	0,0276	0,9725	cereb ix
9509	0,4679	0,0036	-0,0200	0,0500	0,9725	R intraparietal sulcus, pars orbitalis
9670	0,6225	0,0445	0,0301	0,0340	0,9725	ventrolat. PFC ctx
9576	0,5296	-0,0358	-0,0011	-0,0434	0,9725	ant. insula d.
9310	0,3104	0,0232	-0,0051	0,0699	0,9725	dorsomedial PFC ctx ant.
9153	0,2142	-0,0003	-0,0230	0,0856	0,9725	mid. frontal gyr. ant.
9667	0,6194	-0,0018	0,0152	-0,0343	0,9725	R inf. frontal sulcus
9663	0,6153	0,0141	-0,0211	0,0347	0,9725	frontal pole lat.
9573	0,5267	0,0028	0,0897	-0,0437	0,9725	somatomot. net. dorsolat.
9787	0,7469	0,0337	-0,0104	0,0223	0,9725	d. visual stream
9350	0,3389	-0,0133	0,0314	-0,0659	0,9725	parieto occipital sulcus
9453	0,4196	-0,0176	0,0345	-0,0556	0,9725	lat. visual net. post.
9641	0,5931	-0,0300	-0,0216	0,0369	0,9725	presupplementary mot. ctx
9947	0,9278	0,0092	-0,0227	0,0063	0,9734	sup. frontal gyr. ant.
9899	0,8727	0,0573	0,0463	-0,0111	0,9734	sup. parietal lobule
9509	0,4679	0,0347	-0,0419	0,0500	0,9725	L intraparietal sulcus, mid. frontal gyr. post.
9937	0,9163	0,0213	0,0135	-0,0073	0,9734	mid. temporal gyr. post.

**Table S2.6** Difference in individual similarity with 22q11.2 deletion FC-signature in individuals with idiopathic ADHD and controls

U	p_value	median_ADHD	median_Control	rank_biserial_correlation	q_value	node_name
9665	0,6174	-0,0189	-0,0048	0,0345	0,8781	putamen
9816	0,7790	0,0092	0,0003	0,0194	0,8781	post. insula v.
9099	0,1867	0,0323	-0,0168	0,0910	0,8725	cereb vermis
9572	0,5258	-0,0030	0,0652	-0,0438	0,8781	thalamus
8770	0,0722	-0,0392	0,0456	-0,1239	0,6669	cereb viiiab
9970	0,9543	-0,0170	-0,0083	-0,0040	0,9695	cereb i-v
8552	0,0345	0,0742	-0,0120	0,1457	0,6063	ant. cingulate ctx d.
9765	0,7229	-0,0175	0,0083	-0,0245	0,8781	caudate nucleus head, nucleus accumbens
9215	0,2492	-0,0205	0,0221	-0,0794	0,8725	temporal pole
9664	0,6163	0,0171	-0,0053	0,0346	0,8781	dorsomedial PFC ctx post.
9334	0,3273	0,0038	0,0395	-0,0675	0,8725	cereb crus-II R
8773	0,0729	-0,0327	0,0229	-0,1236	0,6669	cereb crus-I
10005	0,9948	0,0294	0,0195	0,0005	0,9948	L inf. frontal sulcus
9831	0,7957	-0,0074	0,0009	0,0179	0,8781	somatomot. net. ventrolat.
8578	0,0379	-0,0253	0,0256	-0,1431	0,6063	cereb viib
9424	0,3958	-0,0148	0,0011	-0,0585	0,8781	fusiform gyr. medial
9693	0,6462	-0,0052	0,0227	-0,0317	0,8781	caudate nucleus
9362	0,3477	-0,0193	-0,0230	0,0647	0,8725	post. insula d.
9627	0,5791	0,0056	-0,0057	0,0383	0,8781	post. cingulate ctx, precuneus
9085	0,1800	-0,0149	0,0284	-0,0924	0,8725	L inf. parietal lobule
9346	0,3359	0,0280	0,0124	0,0663	0,8725	post. cingulate ctx d.
9371	0,3545	-0,0269	0,0009	-0,0638	0,8725	inf. temporal gyr.
9695	0,6483	-0,0117	-0,0033	0,0315	0,8781	supramarginal gyr.
9566	0,5201	0,0376	-0,0096	0,0444	0,8781	mid. temporal gyr. ant.
9590	0,5429	0,0005	-0,0001	-0,0420	0,8781	amygdala, hippocampus
9864	0,8329	-0,0225	0,0060	-0,0146	0,9035	frontal eye field
9591	0,5439	-0,0155	-0,0006	-0,0419	0,8781	visual net. mediod.
9487	0,4486	0,0007	0,0130	-0,0522	0,8781	occipitotemporal gyr. lat.
8297	0,0130	-0,0262	0,0371	-0,1711	0,6063	cereb vi
8742	0,0660	-0,0271	0,0182	-0,1267	0,6669	post. visual net. medial
9898	0,8715	-0,0008	0,0014	-0,0112	0,9144	R inf. parietal lobule
9276	0,2874	0,0065	-0,0256	0,0733	0,8725	inf. marginal sulcus
9298	0,3021	-0,0164	0,0049	-0,0711	0,8725	medial visual net. post.
9653	0,6052	0,0132	0,0116	0,0357	0,8781	perigenual ant. cingulate ctx
9643	0,5951	0,0063	0,0117	-0,0367	0,8781	medial visual net. ant.
9552	0,5070	-0,0065	-0,0048	-0,0458	0,8781	ant. insula v., peri insular sulcus
9485	0,4469	-0,0378	0,0128	-0,0524	0,8781	precuneus d.
9252	0,2720	-0,0189	0,0154	-0,0757	0,8725	lat. visual net. ant.
8956	0,1266	0,0050	-0,0187	0,1053	0,8148	R mid. frontal gyr. post.
8960	0,1280	-0,0250	-0,0015	-0,1049	0,8148	fusiform gyr. lat.
9882	0,8533	0,0174	-0,0081	-0,0128	0,9102	orbitofrontal ctx
9725	0,6799	-0,0096	0,0225	-0,0285	0,8781	v. medial PFC ctx
8578	0,0379	-0,0595	0,0081	-0,1431	0,6063	post. visual net. lat.
9205	0,2433	-0,0085	0,0430	-0,0804	0,8725	cereb crus-II L
9922	0,8990	0,0026	0,0212	0,0088	0,9280	somatomot. net. medial
9809	0,7712	-0,0016	0,0047	-0,0201	0,8781	auditory net.
9770	0,7283	-0,0118	0,0096	-0,0240	0,8781	postcentral sulcus
9181	0,2296	-0,0101	0,0251	-0,0828	0,8725	cereb ix
9234	0,2607	-0,0099	-0,0353	0,0775	0,8725	R intraparietal sulcus, pars orbitalis
9708	0,6619	-0,0056	-0,0181	0,0302	0,8781	ventrolat. PFC ctx
9802	0,7635	-0,0009	-0,0088	-0,0208	0,8781	ant. insula d.
9537	0,4932	0,0138	-0,0028	0,0473	0,8781	dorsomedial PFC ctx ant.
9336	0,3287	0,0157	-0,0278	0,0673	0,8725	mid. frontal gyr. ant.
9770	0,7283	-0,0117	-0,0090	0,0240	0,8781	R inf. frontal sulcus
9823	0,7868	-0,0124	-0,0346	-0,0187	0,8781	frontal pole lat.
9636	0,5881	0,0083	0,0104	0,0374	0,8781	somatomot. net. dorsolat.
9729	0,6842	0,0012	0,0124	-0,0281	0,8781	d. visual stream
9427	0,3982	-0,0082	-0,0303	0,0582	0,8781	parieto occipital sulcus
8837	0,0891	-0,0316	-0,0100	-0,1172	0,7125	lat. visual net. post.
9302	0,3049	-0,0005	-0,0205	0,0707	0,8725	presupplementary mot. ctx
9824	0,7879	0,0286	-0,0227	0,0186	0,8781	sup. frontal gyr. ant.
8992	0,1400	0,0014	0,0435	-0,1017	0,8148	sup. parietal lobule
9710	0,6640	0,0149	0,0000	0,0300	0,8781	L intraparietal sulcus, mid. frontal gyr. post.
9791	0,7513	0,0157	-0,0070	-0,0219	0,8781	mid. temporal gyr. post.



**Table S3.1** Correlation of individual similarity with 16p11.2 deletion FC-signature and FSIQ in ASD

pearson_r	p_value	q_value	node_name
-0,0811	0,0839	0,1411	putamen
-0,0163	0,7292	0,8102	thalamus
-0,0554	0,2381	0,3401	temporal pole
-0,0866	0,0649	0,1411	somatomot. net. ventrolat.
-0,1112	0,0177	0,1217	caudate nucleus
0,0470	0,3172	0,3965	post. cingulate ctx, precuneus
-0,1005	0,0322	0,1217	perigenual ant. cingulate ctx
0,0035	0,9400	0,9400	v. medial PFC ctx
-0,0981	0,0365	0,1217	cereb crus-II L
-0,0809	0,0847	0,1411	ant. insula d.

**Table S3.2** Correlation of individual similarity with 22q11.2 deletion FC-signature and FSIQ in ASD

pearson_r	p_value	q_value	node_name
-0,1033	0,0276	0,0829	putamen
-0,0518	0,2700	0,3375	thalamus
-0,1068	0,0226	0,0829	temporal pole
-0,0742	0,1139	0,1898	somatomot. net. ventrolat.
-0,0344	0,4648	0,5164	caudate nucleus
-0,0654	0,1639	0,2341	post. cingulate ctx, precuneus
-0,1263	0,0070	0,0697	perigenual ant. cingulate ctx
-0,0999	0,0332	0,0829	v. medial PFC ctx
-0,0891	0,0575	0,1150	cereb crus-II L
0,0014	0,9754	0,9754	ant. insula d.

**Table S3.3** Correlation of individual similarity with 16p11.2 deletion FC-signature and ADOS severity in ASD

pearson_r	p_value	q_value	node_name
0,1559	0,0175	0,0584	putamen
0,1006	0,1266	0,2110	thalamus
-0,0283	0,6684	0,7427	temporal pole
0,1437	0,0287	0,0717	somatomot. net. ventrolat.
0,1896	0,0038	0,0375	caudate nucleus
-0,0934	0,1563	0,2233	post. cingulate ctx, precuneus
0,1623	0,0133	0,0584	perigenual ant. cingulate ctx
-0,0804	0,2225	0,2782	v. medial PFC ctx
-0,0193	0,7695	0,7695	cereb crus-II L
0,1206	0,0667	0,1335	ant. insula d.

**Table S3.4** Correlation of individual similarity with 22q11.2 deletion FC-signature and ADOS severity in ASD

pearson_r	p_value	q_value	node_name
0,1315	0,0455	0,0910	putamen
0,1481	0,0241	0,0601	thalamus
0,1859	0,0045	0,0450	temporal pole
0,0562	0,3940	0,4378	somatomot. net. ventrolat.
0,0809	0,2197	0,3139	caudate nucleus
0,1572	0,0165	0,0551	post. cingulate ctx, precuneus
0,1633	0,0127	0,0551	perigenual ant. cingulate ctx
0,1231	0,0613	0,1021	v. medial PFC ctx
0,0650	0,3244	0,4055	cereb crus-II L
0,0295	0,6551	0,6551	ant. insula d.



